Biochemical and Biophysical Research Communications 440 (2013) 515–520

Contents lists available at ScienceDirect

Biochemical and Biophysical Research Communications

journal homepage: www.elsevier.com/locate/ybbrc

Specific inhibition of hepatitis C virus entry into host hepatocytes by fungi-derived sulochrin and its derivatives

Syo Nakajima [a,b], Koichi Watashi [a,b,*], Shinji Kamisuki [b], Senko Tsukuda [a,c], Kenji Takemoto [b], Mami Matsuda [a], Ryosuke Suzuki [a], Hideki Aizaki [a], Fumio Sugawara [b], Takaji Wakita [a]

[a] Department of Virology II, National Institute of Infectious Diseases, Tokyo 162-8640, Japan
[b] Tokyo University of Science Graduate School of Science and Technology, Noda 278-8510, Japan
[c] Micro-Signaling Regulation Technology Unit, RIKEN Center for Life Science Technologies, Wako 351-0198, Japan

ARTICLE INFO

Article history:
Received 5 September 2013
Available online 5 October 2013

Keywords:
HCV
Entry
Sulochrin
Natural product
Screening
Compound

ABSTRACT

Hepatitis C virus (HCV) is a major causative agent of hepatocellular carcinoma. Although various classes of anti-HCV agents have been under clinical development, most of these agents target RNA replication in the HCV life cycle. To achieve a more effective multidrug treatment, the development of new, less expensive anti-HCV agents that target a different step in the HCV life cycle is needed. We prepared an in-house natural product library consisting of compounds derived from fungal strains isolated from seaweeds, mosses, and other plants. A cell-based functional screening of the library identified sulochrin as a compound that decreased HCV infectivity in a multi-round HCV infection assay. Sulochrin inhibited HCV infection in a dose-dependent manner without any apparent cytotoxicity up to 50 μM. HCV pseudoparticle and trans-complemented particle assays suggested that this compound inhibited the entry step in the HCV life cycle. Sulochrin showed anti-HCV activities to multiple HCV genotypes 1a, 1b, and 2a. Co-treatment of sulochrin with interferon or a protease inhibitor telaprevir synergistically augmented their anti-HCV effects. Derivative analysis revealed anti-HCV compounds with higher potencies (IC_{50} < 5 μM). This is the first report showing an antiviral activity of methoxybenzoate derivatives. Thus, sulochrin derivatives are anti-HCV lead compounds with a new mode of action.

1. Introduction

Hepatitis C virus (HCV) infection is a major causative agent of chronic liver diseases such as liver cirrhosis and hepatocellular carcinoma [1]. The standard anti-HCV therapy has been a co-treatment with pegylated-interferon (IFN)α and ribavirin, but this therapy is limited by less efficacy to certain HCV genotypes, poor tolerability, serious side effects, and high cost [2,3]. In addition to the newly approved protease inhibitors, telaprevir and boceprevir, a variety of anti-HCV candidates are under clinical development. Although these drugs improve the virological response rate, the emergence of drug-resistant virus is expected to be a significant problem. Moreover, these compounds are expensive due to their complex structure and the many steps required for their total synthesis. To overcome the drug-resistant virus and achieve a long-term antiviral effect, multidrug treatment is essential. Thus, the development of drugs targeting a different step in the HCV life cycle and presumably requiring low cost is urgently needed.

HCV propagates in hepatocytes through its viral life cycle including: attachment and entry (defined as the early step in this study); translation, polyprotein processing, and RNA replication (the middle step); and assembly, trafficking, budding, and release (the late step) (Supplementary Fig. S1). The middle step has been extensively analysed, especially after the establishment of the HCV replicon system [4]. The early step can be analysed with HCV pseudoparticle (HCVpp) [5,6], which is a murine leukemia virus- or human immunodeficiency virus-based pseudovirus carrying HCV E1 and E2 as envelope proteins. The HCV-producing cell culture system (HCVcc) is used for analyzing the whole life cycle [7–9]. In addition, the HCV trans-complemented particle (HCVtcp) system carrying an HCV subgenomic replicon RNA packaged in HCV E1 and E2-containing particles can evaluate the life cycle from the early to the middle step [10]. The majority of anti-HCV agents currently under clinical development, such as inhibitors of protease, polymerase, NS5A, and cellular cyclophilin, inhibit polyprotein processing and/or RNA replication. A desirable approach

Abbreviations: HCV, hepatitis C virus; IFN, interferon; HCVpp, HCV pseudoparticle; HCVcc, HCV derived from cell culture; HCVtcp, HCV trans-complemented particle; MOI, multiplicity of infection; HBs, HBV envelope protein; CsA, cyclosporin A; VSV, vesicular stomatitis virus.

* Corresponding author. Adress: Department of Virology II, National Institute of Infectious Diseases, 1-23-1 Toyama, Shinjuku-ku, Tokyo 162-8640, Japan. Fax: +81 3 5285 1161.
E-mail address: kwatashi@nih.go.jp (K. Watashi).

0006-291X/$ - see front matter © 2013 Elsevier Inc. All rights reserved.
http://dx.doi.org/10.1016/j.bbrc.2013.09.100

to achieving efficient multidrug therapy is to identify new antiviral drugs targeting different steps in the viral life cycle. A combination of drugs with different targets can greatly decrease the emergence of drug-resistant virus.

Natural products generally contain more characteristics of high chemical diversity than combinatorial chemical collections, and therefore have a wider range of physiological activities [11,12]. They offer major opportunities for finding novel lead structures that are active in a biological assay. Moreover, biologically active natural products are generally small molecules with drug-like properties, and thus development costs of producing orally active agents tend to be lower than that derived from combinatorial chemistry [13]. In addition, there is a wide variety of natural compounds reported to possess antiviral activity [14,15]. In the present study, we have taken advantage of the potential of natural products by screening a natural product library derived from fungal extracts with a cell-based assay that supports the whole life cycle of HCV.

2. Materials and methods

2.1. Cell culture

Huh-7.5.1 [8] and HepaRG cells [16] were cultured as described previously.

2.2. Natural product library and reagents

Natural products were extracted essentially as previously described [17]. Culture broths of fungal strains isolated from seaweeds, mosses, and other plants were extracted with CH_2Cl_2. The crude extracts were separated by silica gel column chromatography to purify compounds. The chemical structure of each compound was determined by NMR and mass spectrometry analyses. Thus, we prepared an in-house natural product library consisting of approximately 300 isolated compounds.

Cyclosporin A was purchased from Sigma. Bafilomycin A1 and chlorpromazine were purchased from Wako. Heparin was obtained from Mochida Pharmaceutical. IFNα was purchased from Schering-Plough.

2.3. Compound screening

Huh-7.5.1 cells were treated with HCV J6/JFH1 at a multiplicity of infection (MOI) of 0.15 for 4 h. The cells were washed and then cultured with growth medium treated with 10 μM of each compound for 72 h. The infectivity of HCV in the medium was quantified. Cell viability at 72 h post-treatment was simultaneously measured. Compounds that decreased the cell viability to less than 50% of that without treatment were eliminated for further evaluations. Normalised infectivity was calculated as HCV infectivity divided by cell viability. Compounds reducing the normalised infectivity to less than 40% were selected as initial hits. The initial hits were further evaluated for data reproduction and dose-dependency.

2.4. HCVcc assay

HCVcc was recovered from the medium of Huh-7.5.1 cells transfected with HCV J6/JFH-1 RNA as described [7]. HCVcc was infected into Huh-7.5.1 cells at 0.15 MOI for 4 h. After washing out the inoculated virus, the cells were cultured with normal growth medium in the presence or absence of compounds for 72 h. The infectivity of HCV and the amount of HCV core protein in the medium were quantified by infectious focus formation assay and chemiluminescent enzyme immunoassay (Lumipulse II HCV core assay, ortho clinical diagnostics), respectively [7,18].

2.5. Immunoblot analysis

Immunoblot analysis was performed as described previously [19]. The anti-HCV core antibody (2H9) was used as a primary antibody with 1:1000 dilution [7].

2.6. MTT assay

The viability of cells was quantified by using a Cell Proliferation Kit II XTT (Roche Diagnostics) as described previously [20].

2.7. HCV replicon assay

Huh-7.5.1 cells were transfected with an HCV subgenome replicon RNA (SGR-JFH1/Luc) for 4 h and then incubated with or without compounds for 48 h [21]. The cells were lysed with 1xPLB (Promega), and the luciferase activity was determined with a luciferase assay system (Promega) according to the manufacturer's protocol [22].

2.8. HCVpp assay

HCVpp was recovered from the medium of 293T cells transfected with expression plasmids for HCV JFH-1 E1E2, MLV Gag-Pol, and luciferase, which were kindly provided from Dr. Francois-Loic Cosset at Universite de Lyon [5]. Vesicular stomatitis virus pseudoparticles (VSVpp) was similarly recovered with transfection by replacing HCV E1E2 with VSV G.

Huh-7.5.1 cells were preincubated with compounds for 3 h and were then infected with HCVpp in the presence of compounds for 4 h. After washing out virus and compounds, cells were incubated for an additional 72 h before recovering the cell lysates and quantifying the luciferase activity.

2.9. HCVtcp assay

The HCVtcp assay was essentially performed as described [10]. Briefly, Huh-7 cells were transfected with expression plasmids for the HCV subgenomic replicon carrying the luciferase gene and for HCV core-NS2 based on genotype 1a (RMT) (kindly provided by Dr. Michinori Kohara at Tokyo Metropolitan Institute of Medical Science), 1b (Con1), and 2a (JFH-1) [4,10,23] to recover HCVtcp. HCVtcp can reproduce RNA replication as well as HCV-mediated entry into the cells [10].

2.10. Synergy analysis

To determine whether the effect of the drug combination was synergistic, additive, or antagonistic, MacSynergy (kindly provided by Mark Prichard), a mathematical model based on the Bliss independence theory, was used to analyse the experimental data shown in Fig. 3A. In this model, a theoretical additive effect with any given concentrations can be calculated by $Z = X + Y(1-X)$, where X and Y represent the inhibition produced by each drug alone, and Z represents the effect produced by the combination of two compounds if they were additive. The theoretical additive effects were compared to the actual experimental effects at various concentrations of the two compounds and were plotted as a three-dimensional differential surface that would appear as a horizontal plane at 0 if the combination were additive. Any peak above this plane (positive values) indicates synergy, whereas any depression below the plane (negative values) indicates antagonism. The 95% confidence interval of the experimental dose–response was considered to reveal only effects that were statistically significant.

3. Results

3.1. Screening of natural products possessing anti-HCV activity

We extracted culture broths of fungal strains isolated from seaweeds, mosses, and other plants and purified compounds as described in the Section 2 [17]. The chemical structure of each compound was determined by NMR and mass spectrometry analyses. Thus, we prepared an in-house natural product library consisting of approximately 300 isolated compounds. As shown in the Section 2, compounds reducing the normalised HCV infectivity to less than 40% as compared with DMSO were selected as primary hits. The primary hits were then validated by examining the reproducibility, dose-dependency, and cell viability in the HCVcc system. Sulochrin [methyl 2-(2,6-dihydroxy-4-methylbenzoyl)-5-hydroxy-3-methoxybenzoate] (Fig. 1A) was one of the compounds showing the highest anti-HCV activity, and the following analyses focus mainly on this compound.

3.2. Sulochrin decreased HCV infectivity in HCV cell culture assay

To characterise the anti-HCV activity of the compounds, Huh-7.5.1 cells were infected with HCV J6/JFH1 at an MOI of 0.15 and then cultured for 72 h in the presence or absence of compounds.

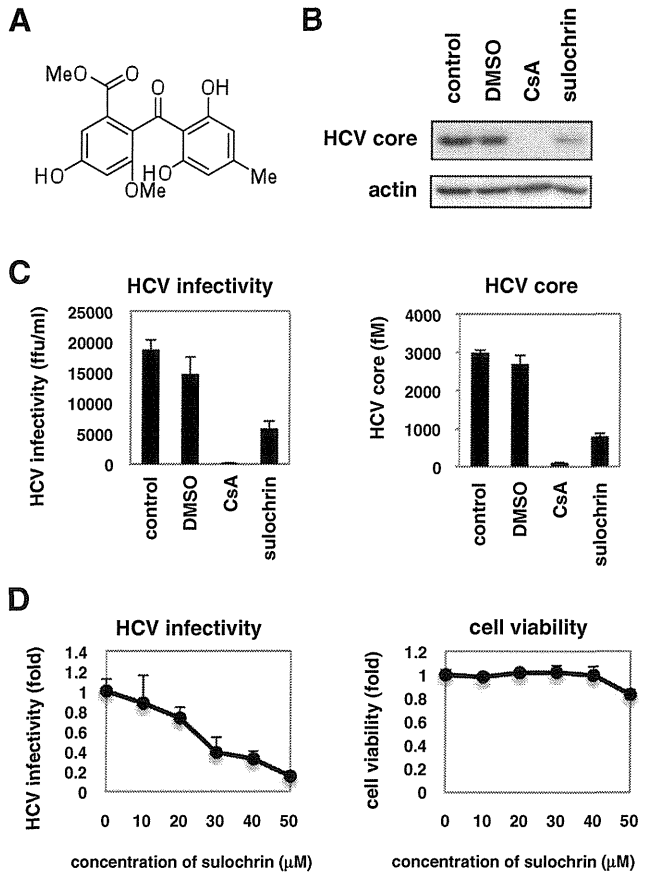

Fig. 1. Sulochrin decreased HCV production in a multi-round HCV infection assay. (A) Chemical structure of sulochrin. (B) Huh-7.5.1 cells were infected with HCV J6/JFH-1 at an MOI of 0.15 for 4 h and then incubated with or without 0.3% DMSO, 2 μM cyclosporin A (CsA), or 30 μM sulochrin for 72 h. The resultant medium was inoculated into naïve Huh-7.5.1 cells to detect intracellular HCV core and actin protein at 48 h postinoculation by immunoblot. (C) HCV infectivity (left) and HCV core protein (right) in the medium as prepared in (B) were quantified as shown in the Section 2. (D) HCV infectivity (left) determined as shown in (C) with varying concentrations (0–50 μM) of sulochrin. Cell viability was examined by MTT assay (right).

In this system, infectious HCV is secreted into the medium and then re-infects into uninfected cells to support the spread of HCV during a 72 h period (Section 2). Cell cultures were treated with sulochrin or cyclosporin A (CsA) as a positive control in this mul-

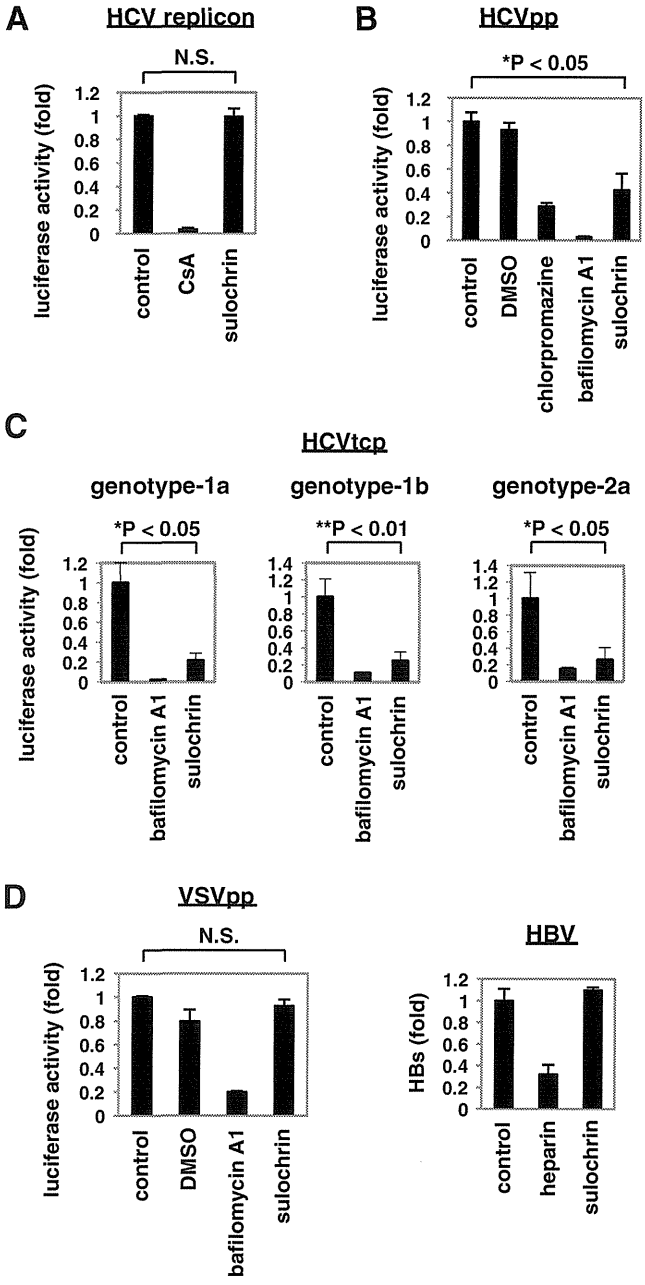

Fig. 2. Sulochrin blocked HCV entry. (A) Replicon assay. Huh-7.5.1 cells were transfected with an HCV subgenomic replicon RNA for 4 h followed by treatment with or without the indicated compounds for 48 h. Luciferase activity driven by the replication of the subgenomic replicon was quantified. (B and C) HCV pseudoparticle (HCVpp) and trans-complemented particle (HCVtcp) assay. Huh-7.5.1 cells were pretreated with the indicated compounds for 3 h and then infected with HCVpp (B) or HCVtcp (C) for 4 h. After washing out virus and compounds, cells were further incubated for 72 h and harvested for measuring luciferase activity driven by the infection of HCVpp or HCVtcp. HCVtcp assay was performed with HCV E1 and E2 derived from genotypes 1a (RMT), 1b (Con1), and 2a (JFH1). (D) Left, the pseudoparticle assay was performed as shown in (B) with VSV G instead of HCV E1 and E2. Right, HBV infection assay. HepaRG cells were pretreated with the indicated compounds for 3 h and then infected with HBV for 16 h. After washing out virus and compounds, cells were incubated for an additional 12 days. HBV infection was evaluated by measuring HBs secretion from the infected cells. Heparin was used as a positive control that inhibits HBV entry.

ti-round infection system. To examine the level of infectious HCV particles produced from the cells, the resultant medium was inoculated into naive Huh-7.5.1 cells to detect HCV core protein in the cells. As shown in Fig. 1B, intracellular production of HCV core but not that of actin was reduced in the cells inoculated with sulochrin- and CsA-treated medium (Fig. 1B). Quantitative analysis showed that sulochrin decreased HCV infectivity and HCV core protein in the medium to 1/3–1/4 of the untreated levels (Fig. 1C). Reduction of HCV infectivity by sulochrin was dose-dependent without serious cytotoxicity up to 50 μM (Fig. 1D).

3.3. Sulochrin blocked HCV entry

We investigated the step in the HCV life cycle that was inhibited by sulochrin. The middle step of the life cycle including translation and RNA replication was evaluated with the transient replication assay by using the HCV subgenomic replicon. Sulochrin had little effect on the replicon activity at doses up to 50 μM (Fig. 2A). In the HCVpp system, which reproduced the early step of HCV infection including entry, sulochrin significantly inhibited HCVpp infection (Fig. 2B). Sulochrin also inhibited the infection of HCVtcp, which reproduced both the viral entry and RNA replication, further supporting that this compound targeted the entry step (Fig. 2C). In contrast, VSV G-mediated viral entry efficiency was not altered by sulochrin treatment (Fig. 2D). Additionally, HBV entry was not inhibited by the presence of sulochrin (Fig. 2D). These data suggest that the inhibitory activity of sulochrin on viral entry is specific to HCV. The anti-HCV entry activity of sulochrin was conserved among different HCV genotypes, 1a (RMT), 1b (Con1), and 2a (JFH-1) [4,10,23] (Fig. 2C).

3.4. Synergistic effect of cotreatment of sulochrin with IFNα or telaprevir

We examined the anti-HCV activity of sulochrin co-administered with clinically available anti-HCV agents, IFNα and a prote-

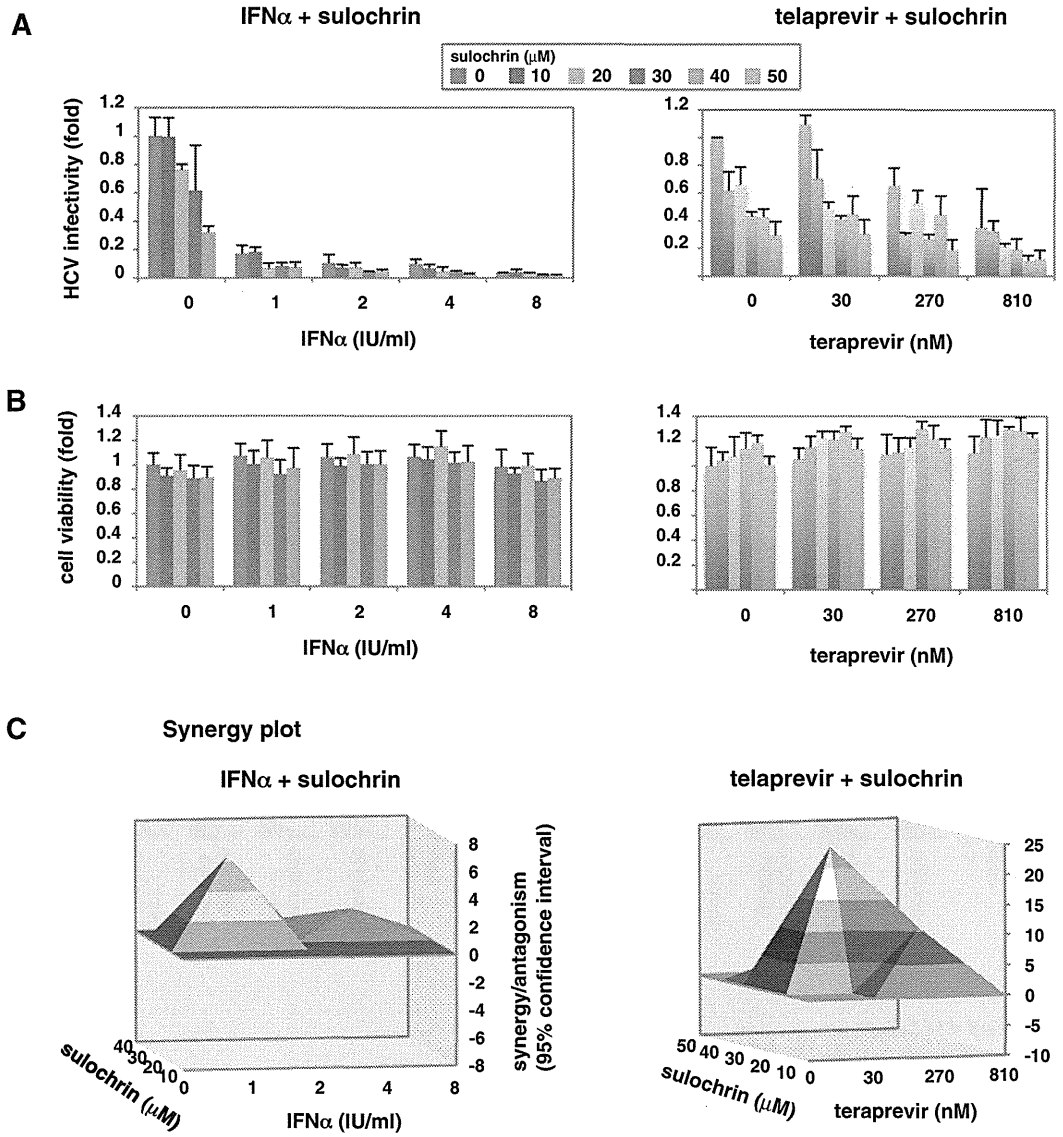

Fig. 3. Cotreatment of sulochrin with IFNα or telaprevir. (A, B) Huh-7.5.1 cells infected with HCV were treated with the indicated concentrations of sulochrin with IFNα (left) or telaprevir (right) to determine HCV infectivity in the medium (A) as shown in Fig. 1C. Cell viability was also quantified (B). (C) Synergy analysis. The results of the combinations shown in (A) were analysed with a mathematical model, MacSynergy, as described in the Section 2. The three-dimensional surface plot represents the difference between actual experimental effects and theoretical additive effects of the combination treatment (95% confidence interval). The theoretical additive effects are shown as the zero plane (dark gray) across the *z*-axis. A positive value in the *z*-axis as a peak above the plane indicates synergy, and a negative value with a valley below the plane indicates antagonism. Sulochrin in combination with IFNα (left) or telaprevir (right) produced synergistic antiviral effects that were greater than the theoretical additive effects.

ase inhibitor telaprevir. As shown in Fig. 3, addition of sulochrin with IFNα or telaprevir led to a further decrease in HCV infectivity (Fig. 3A) without significantly enhancing cytotoxicity (Fig. 3B) at any given concentrations. Thus, the combination of sulochrin and IFNα or telaprevir always resulted in a greater reduction in HCV infectivity as compared with that achieved by either agent alone. Synergy/antagonism analysis with the Bliss independence model showed that the experimental anti-HCV activity in combination with sulochrin and IFNα or telaprevir showed a peak above the zero plane in the *z*-axis, which shows the calculated theoretical additive effect (Fig. 3C). Any peak above the zero plane indicates more than an additive effect, namely, synergy (Section 2). The data clearly indicate that sulochrin had a synergistic anti-HCV effect with both IFNα and telaprevir.

3.5. Derivative analysis of sulochrin

We examined the anti-HCV activity of a series of sulochrin derivatives (Fig. 4A) in the HCVcc system. Monochlorosulochrin and dihydrogeodin, mono- or dichloro-substituted derivatives of sulochrin, possessed even higher anti-HCV activity than sulochrin (Fig. 4B and C). Deoxyfunicone, of which one aromatic ring was replaced by a 4-pyrone ring, had approximately 5-fold greater HCV inhibitory activity as compared with sulochrin (Fig. 4B and C). An additional compound, 3-*O*-methylfunicone, also possessed anti-HCV activity (Fig. 4B and C). These data suggest that the 1,3-dihydroxy-5-methylbenzene moiety of sulochrin is important for anti-HCV activity. Furthermore, funicone derivatives as well as sulochrin derivatives are likely to be lead compounds for a new class of anti-HCV agents.

4. Discussion

In the present study, we prepared a natural product library consisting of approximately 300 isolated compounds derived from fungi extract [17]. Among these compounds, we focused on sulochrin, which reduced HCV infectivity in the HCVcc system. Sulochrin suppressed the viral entry efficiencies both in the HCVpp and the HCVtcp systems, suggesting that this compound blocked HCV envelope-mediated entry. HCV was reported to enter host cells through clathrin-dependent endocytosis after engagement to host receptors [24–27]. Sulochrin is not likely to be a general inhibitor of clathrin-dependent endocytosis, but rather is specific for HCV entry, as it did not affect the entry of other viruses such as VSVpp and HBV, which were reported to enter by clathrin-dependent manners [28,29].

Sulochrin inhibits eosinophil degranulation, activation, and chemotaxis [30,31]. It also inhibits VEGF-induced tube formation of human umbilical vein endothelial cells [32]. In addition, 3-*O*-methylfunicone, a sulochrin derivative possessing anti-HCV activity, has an anti-tumor activity [33]. It is unknown if these activities of the compounds are related to their anti-HCV activity. The establishment of drug-resistant virus and the identification of the target molecule are in progress to reveal the mechanism of action of sulochrin and its derivatives. However, the present study is the

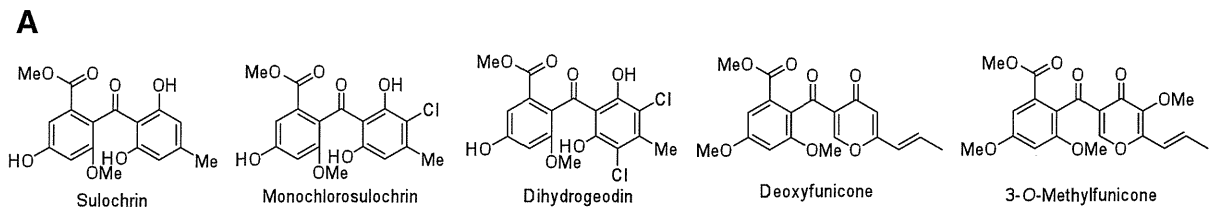

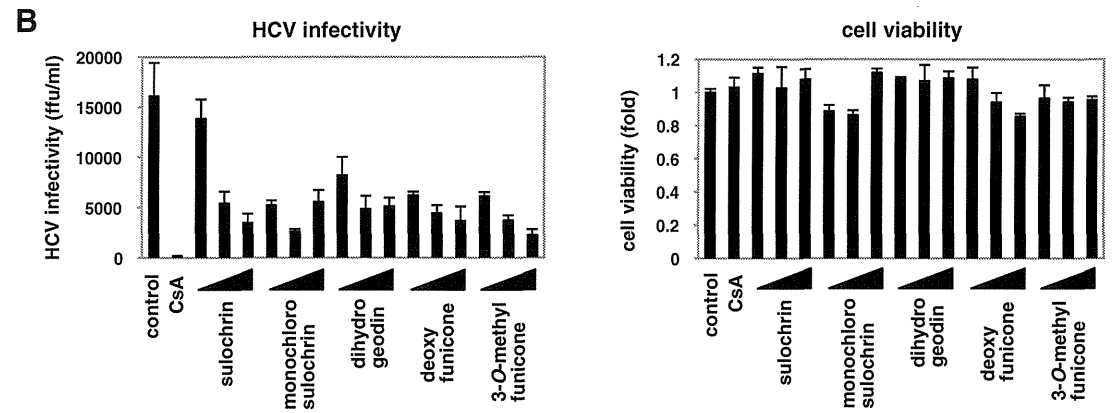

C

IC_{50}s and CC_{50}s

compound	IC_{50} (μM)	CC_{50} (μM)
sulochrin	24.4 ± 2.0	> 50
monochlorosulochrin	4.3 ± 1.1	> 50
dihydrogeodin	10.3 ± 0.3	> 50
deoxyfunicone	4.6 ± 1.1	> 50
3-*O*-methylfunicone	6.2 ± 2.3	> 50

Fig. 4. Derivative analysis of sulochrin. (A) Chemical structures of sulochrin derivatives examined in this study, monochlorosulochrin, dihydrogeodin, deoxyfunicone, 3-*O*-methyfunicone, as well as sulochrin. (B) Anti-HCV effects of the sulochrin derivatives (10, 30, and 50 μM) were investigated as shown in Fig. 1C. (C) The IC_{50} and CC_{50} values of the sulochrin derivatives are shown.

first report to demonstrate the antiviral activity of these compounds. It is important to note that sulochrin inhibited the entry of HCV genotype 1a and b, which are the dominant genotypes in North America, Europe, and East Asia, indicating that this compound has potential clinical applications. Promising applications of entry inhibitors include the prevention of HCV recurrence in patients after liver transplantation. In patients with HCV-related end-stage liver diseases undergoing liver transplantation, re-infection of the graft is universal and characterised by accelerated progression of liver diseases. Entry inhibitors may be effective especially in these conditions under robust re-infection of HCV into hepatocytes. In the present study, we showed that co-treatment of sulochrin with IFNα and a protease inhibitor, teleprevir, synergistically augmented the anti-HCV effects of these approved drugs. These results suggest the possibility that co-treatment with sulochrin and probably its effective derivatives helps to inhibit the spread of HCV infection. We also identified the chemical structure and the derivatives of sulochrin as lead compounds for anti-HCV agents. Further derivatives analysis may identify more preferable anti-HCV agents.

In conclusion, our results demonstrate that sulochrin and its derivatives are potent and selective inhibitors of HCV infection in cell culture. Although further studies including an analysis of mode of action and pharmacological properties *in vivo* are required, this class of compounds should be pursued for its clinical potential in the treatment of HCV infection.

Acknowledgments

Huh-7.5.1 cells were kindly provided by Dr. Francis Chisari at The Scripps Research Institute. The expression plasmids for producing HCVpp were a generous gift from Dr. Francois-Loic Cosset at Universite de Lyon. The expression plasmid for HCV E1E2 of genotype 1a (RMT) was kindly provided by Dr. Michinori Kohara at Tokyo Metropolitan Institute of Medical Science. We thank all of the members of the Department of Virology II, National Institute of Infectious Diseases, for their helpful discussions. This study was supported by grants-in-aid from the Ministry of Health, Labour, and Welfare, Japan, from the Ministry of Education, Culture, Sports, Science, and Technology, Japan, and from the Japan Society for the Promotion of Science.

Appendix A. Supplementary data

Supplementary data associated with this article can be found, in the online version, at http://dx.doi.org/10.1016/j.bbrc.2013.09.100.

References

[1] T.J. Liang, V. Rustgi, E. Galun, H.E. Blum, HCV RNA in patients with chronic hepatitis C treated with interferon-alpha, J. Med. Virol. 40 (1993) 69–75.
[2] J.G. McHutchison, S.C. Gordon, E.R. Schiff, M.L. Shiffman, W.M. Lee, V.K. Rustgi, Z.D. Goodman, M.H. Ling, S. Cort, J.K. Albrecht, Interferon alfa-2b alone or in combination with ribavirin as initial treatment for chronic hepatitis C. Hepatitis interventional therapy group, N. Engl. J. Med. 339 (1998) 1485–1492.
[3] A.W. Tai, R.T. Chung, Treatment failure in hepatitis C: mechanisms of non-response, J. Hepatol. 50 (2009) 412–420.
[4] V. Lohmann, F. Korner, J. Koch, U. Herian, L. Theilmann, R. Bartenschlager, Replication of subgenomic hepatitis C virus RNAs in a hepatoma cell line, Science 285 (1999) 110–113.
[5] B. Bartosch, J. Dubuisson, F.L. Cosset, Infectious hepatitis C virus pseudo-particles containing functional E1–E2 envelope protein complexes, J. Exp. Med. 197 (2003) 633–642.
[6] M. Hsu, J. Zhang, M. Flint, C. Logvinoff, C. Cheng-Mayer, C.M. Rice, J.A. McKeating, Hepatitis C virus glycoproteins mediate pH-dependent cell entry of pseudotyped retroviral particles, Proc. Natl. Acad. Sci. USA 100 (2003) 7271–7276.
[7] T. Wakita, T. Pietschmann, T. Kato, T. Date, M. Miyamoto, Z. Zhao, K. Murthy, A. Habermann, H.G. Krausslich, M. Mizokami, R. Bartenschlager, T.J. Liang, Production of infectious hepatitis C virus in tissue culture from a cloned viral genome, Nat. Med. 11 (2005) 791–796.
[8] J. Zhong, P. Gastaminza, G. Cheng, S. Kapadia, T. Kato, D.R. Burton, S.F. Wieland, S.L. Uprichard, T. Wakita, F.V. Chisari, Robust hepatitis C virus infection *in vitro*, Proc. Natl. Acad. Sci. USA 102 (2005) 9294–9299.
[9] B.D. Lindenbach, M.J. Evans, A.J. Syder, B. Wolk, T.L. Tellinghuisen, C.C. Liu, T. Maruyama, R.O. Hynes, D.R. Burton, J.A. McKeating, C.M. Rice, Complete replication of hepatitis C virus in cell culture, Science 309 (2005) 623–626.
[10] R. Suzuki, K. Saito, T. Kato, M. Shirakura, D. Akazawa, K. Ishii, H. Aizaki, Y. Kanegae, Y. Matsuura, I. Saito, T. Wakita, T. Suzuki, Trans-complemented hepatitis C virus particles as a versatile tool for study of virus assembly and infection, Virology 432 (2012) 29–38.
[11] G.M. Cragg, D.J. Newman, Natural products: a continuing source of novel drug leads, Biochim. Biophys. Acta 2013 (1830) 3670–3695.
[12] D.J. Newman, G.M. Cragg, Natural products as sources of new drugs over the 30 years from 1981 to 2010, J. Nat. Prod. 75 (2012) 311–335.
[13] A.L. Harvey, Natural products as a screening resource, Curr. Opin. Chem. Biol. 11 (2007) 480–484.
[14] S.S. Yang, G.M. Cragg, D.J. Newman, J.P. Bader, Natural product-based anti-HIV drug discovery and development facilitated by the NCI developmental therapeutics program, J. Nat. Prod. 64 (2001) 265–277.
[15] K. Kitazato, Y. Wang, N. Kobayashi, Viral infectious disease and natural products with antiviral activity, Drug Discovery Ther. 1 (2007) 14–22.
[16] K. Watashi, G. Liang, M. Iwamoto, H. Marusawa, N. Uchida, T. Daito, K. Kitamura, M. Muramatsu, H. Ohashi, T. Kiyohara, R. Suzuki, J. Li, S. Tong, Y. Tanaka, K. Murata, H. Aizaki, T. Wakita, Interleukin-1 and tumor necrosis factor-alpha trigger restriction of hepatitis B virus infection via a cytidine deaminase AID, J. Biol Chem. PMID: 24025329.
[17] Y. Myobatake, T. Takeuchi, K. Kuramochi, I. Kuriyama, T. Ishido, K. Hirano, F. Sugawara, H. Yoshida, Y. Mizushina, Pinophilins A and B, inhibitors of mammalian A-, B-, and Y-family DNA polymerases and human cancer cell proliferation, J. Nat. Prod. 75 (2012) 135–141.
[18] A. Murayama, N. Sugiyama, K. Watashi, T. Masaki, R. Suzuki, H. Aizaki, T. Mizuochi, T. Wakita, T. Kato, Japanese reference panel of blood specimens for evaluation of hepatitis C virus RNA and core antigen quantitative assays, J. Clin. Microbiol. 50 (2012) 1943–1949.
[19] K. Watashi, M. Khan, V.R. Yedavalli, M.L. Yeung, K. Strebel, K.T. Jeang, Human immunodeficiency virus type 1 replication and regulation of APOBEC3G by peptidyl prolyl isomerase Pin1, J. Virol. 82 (2008) 9928–9936.
[20] K. Watashi, M.L. Yeung, M.F. Starost, R.S. Hosmane, K.T. Jeang, Identification of small molecules that suppress microRNA function and reverse tumorigenesis, J. Biol. Chem. 285 (2010) 24707–24716.
[21] T. Kato, T. Date, M. Miyamoto, M. Sugiyama, Y. Tanaka, E. Orito, T. Ohno, K. Sugihara, I. Hasegawa, K. Fujiwara, K. Ito, A. Ozasa, M. Mizokami, T. Wakita, Detection of anti-hepatitis C virus effects of interferon and ribavirin by a sensitive replicon system, J. Clin. Microbiol. 43 (2005) 5679–5684.
[22] H. Marusawa, M. Hijikata, K. Watashi, T. Chiba, K. Shimotohno, Regulation of Fas-mediated apoptosis by NF-kappa B activity in human hepatocyte derived cell lines, Microbiol. Immunol. 45 (2001) 483–489.
[23] F. Yasui, M. Sudoh, M. Arai, M. Kohara, Synthetic lipophilic antioxidant BO-653 suppresses HCV replication, J. Med. Virol. 85 (2013) 241–249.
[24] M.B. Zeisel, I. Fofana, S. Fafi-Kremer, T.F. Baumert, Hepatitis C virus entry into hepatocytes: molecular mechanisms and targets for antiviral therapies, J. Hepatol. 54 (2011) 566–576.
[25] E. Blanchard, S. Belouzard, L. Goueslain, T. Wakita, J. Dubuisson, C. Wychowski, Y. Rouille, Hepatitis C virus entry depends on clathrin-mediated endocytosis, J. Virol. 80 (2006) 6964–6972.
[26] A. Codran, C. Royer, D. Jaeck, M. Bastien-Valle, T.F. Baumert, M.P. Kieny, C.A. Pereira, J.P. Martin, Entry of hepatitis C virus pseudotypes into primary human hepatocytes by clathrin-dependent endocytosis, J. Gen. Virol. 87 (2006) 2583–2593.
[27] L. Meertens, C. Bertaux, T. Dragic, Hepatitis C virus entry requires a critical postinternalisation step and delivery to early endosomes via clathrin-coated vesicles, J. Virol. 80 (2006) 11571–11578.
[28] D.K. Cureton, R.H. Massol, S.P. Whelan, T. Kirchhausen, The length of vesicular stomatitis virus particles dictates a need for actin assembly during clathrin-dependent endocytosis, PLoS Pathog. 6 (2010) e1001127.
[29] H.C. Huang, C.C. Chen, W.C. Chang, M.H. Tao, C. Huang, Entry of hepatitis B virus into immortalised human primary hepatocytes by clathrin-dependent endocytosis, J. Virol. 86 (2012) 9443–9453.
[30] H. Ohashi, M. Ishikawa, J. Ito, A. Ueno, G.J. Gleich, H. Kita, H. Kawai, H. Fukamachi, Sulochrin inhibits eosinophil degranulation, J. Antibiotechnol. (Tokyo) 50 (1997) 972–974.
[31] H. Ohashi, Y. Motegi, H. Kita, G.J. Gleich, T. Miura, M. Ishikawa, H. Kawai, H. Fukamachi, Sulochrin inhibits eosinophil activation and chemotaxis, Inflamm. Res. 47 (1998) 409–415.
[32] H.J. Lee, J.H. Lee, B.Y. Hwang, H.S. Kim, J.J. Lee, Fungal metabolites, asterric acid derivatives inhibit vascular endothelial growth factor (VEGF)-induced tube formation of HUVECs, J. Antibiotechnol. (Tokyo) 55 (2002) 552–556.
[33] R. Nicoletti, E. Manzo, M.L. Ciavatta, Occurence and bioactivities of funicone-related compounds, Int. J. Mol. Sci. 10 (2009) 1430–1444.

ELSEVIER

Institut Pasteur

Microbes and Infection 15 (2013) 56–65

www.elsevier.com/locate/micinf

Original article

Gag-CA Q110D mutation elicits TRIM5-independent enhancement of HIV-1mt replication in macaque cells

Masako Nomaguchi [a,1], Masaru Yokoyama [b,1], Ken Kono [c], Emi E. Nakayama [c], Tatsuo Shioda [c], Akatsuki Saito [d], Hirofumi Akari [d], Yasuhiro Yasutomi [e], Tetsuro Matano [f], Hironori Sato [b], Akio Adachi [a,*]

[a] *Department of Microbiology, Institute of Health Biosciences, The University of Tokushima Graduate School, 3-18-15 Kuramoto, Tokushima 770-8503, Japan*
[b] *Laboratory of Viral Genomics, Pathogen Genomics Center, National Institute of Infectious Diseases, 4-7-1 Gakuen, Musashimurayama, Tokyo 208-0011, Japan*
[c] *Department of Viral Infections, Research Institute for Microbial Diseases, Osaka University, 3-1 Yamadaoka, Suita, Osaka 565-0871, Japan*
[d] *Center for Human Evolution Modeling Research, Primate Research Institute, Kyoto University, 41-2 Kanrin, Inuyama, Aichi 484-8506, Japan*
[e] *Tsukuba Primate Research Center, National Institute of Biomedical Innovation, Tsukuba, Ibaraki 305-0843, Japan*
[f] *AIDS Research Center, National Institute of Infectious Diseases, 1-23-1 Toyama, Shinjuku-ku, Tokyo 162-8640, Japan*

Received 5 September 2012; accepted 20 October 2012
Available online 1 November 2012

Abstract

HIV-1 is strictly adapted to humans, and cause disease-inducing persistent infection only in humans. We have generated a series of macaque-tropic HIV-1 (HIV-1mt) to establish non-human primate models for basic and clinical studies. HIV-1mt clones available to date grow poorly in macaque cells relative to SIVmac239. In this study, viral adaptive mutation in macaque cells, G114E in capsid (CA) helix 6 of HIV-1mt, that enhances viral replication was identified. Computer-assisted structural analysis predicted that another Q110D mutation in CA helix 6 would also increase viral growth potential. A new proviral construct MN4Rh-3 carrying CA-Q110D exhibited exquisitely enhanced growth property specifically in macaque cells. Susceptibility of MN4Rh-3 to macaque TRIM5α/TRIMCyp proteins was examined by their expression systems. HIV-1mt clones so far constructed already completely evaded TRIMCyp restriction, and further enhancement of TRIMCyp resistance by Q110D was not observed. In addition, Q110D did not contribute to evasion from TRIM5α restriction. However, the single-cycle infectivity of MN4Rh-3 in macaque cells was enhanced relative to the other HIV-1mt clones. Our results here indicate that CA-Q110D accelerates viral growth in macaque cells irrelevant to TRIM5 proteins restriction.

Keywords: HIV-1; HIV-1mt; Gag-CA; Macaque cells; Virus growth; Molecular modeling

1. Introduction

Mammalian cells express a variety of host restriction factors to defend themselves against pathogens. Viruses have evolved countermeasures to subvert their restriction and replicate efficiently in cells [1,2]. HIV-1, a causative agent of human AIDS, evades host restriction factors and replicates well in human cells. However, in macaques for experimental use, e.g. cynomolgus macaques (CyMs) and rhesus macaques (RhMs), HIV-1 replication is completely inhibited by host restriction factors present in their cells [3]. Construction of HIV-1 that overcomes species-barrier contributes much to understand the interaction of HIV-1 and its host as well as the establishment of HIV-1-infected macaque models [4,5].

Extensive molecular biological studies on the HIV-1/host interaction conducted to date have revealed main mechanical bases for the narrow host range exhibited by HIV-1. Macaque cells contain potent antiviral factors that effectively restrict or even abolish HIV-1 replication. These include APOBEC3 proteins (APOs), CyclophilinA (CypA), and TRIM5α/TRIMCyp

* Corresponding author. Tel.: +81 88 633 7078; fax: +81 88 633 7080.
E-mail address: adachi@basic.med.tokushima-u.ac.jp (A. Adachi).
[1] Masako Nomaguchi and Masaru Yokoyama contributed equally to this work.

1286-4579/$ - see front matter © 2012 Institut Pasteur. Published by Elsevier Masson SAS. All rights reserved.
http://dx.doi.org/10.1016/j.micinf.2012.10.013

(TRIM5 proteins). HIV-1 can indeed counteract human proteins corresponding to these restriction factors. APOs exhibit cytidine deaminase activity, and introduce lethal mutations into HIV-1 genome. HIV-1 Vif is able to neutralize the antiviral activity of human APOs, but not macaque APOs [6–8]. CypA acts on incoming HIV-1 core to regulate infection positively in human cells but negatively in macaque cells [9–11], though amino acid sequences of CypA from human and macaque are identical. Macaque TRIM5α recognizes and interacts with incoming HIV-1 core, and restricts virus infection in a less-defined mechanism [9–11]. Macaque TRIM5α is polymorphic, and has sequence variation in a C-terminal B30.2/SPRY domain important for capsid (CA) binding. Sequence variation in this domain causes modulation of host susceptibility to retrovirus infection [12,13]. Macaque TRIMCyp is a fusion protein resulted from replacement of a B30.2/SPRY domain with CypA. Both CyM and RhM cells express TRIMCyp, but affinity of these proteins to HIV-1 core is different due to amino acid substitutions in Cyp domains. Thus, CyM TRIMCyp restricts HIV-1 replication, but not RhM TRIMCyp [14,15].

Identification of host restriction factors in macaque cells and their target proteins in HIV-1 has prompted us to generate macaque-tropic HIV-1 (HIV-1mt) with a minimal modification of HIV-1 genome. We successfully constructed prototype HIV-1mt, NL-DT5R, by replacing CypA binding region on a loop between helices 4 and 5 (h4/5L) in *gag*-CA and entire *vif* genes with the corresponding regions of pathogenic SIVmac239 (Fig. 1) [16]. But growth potential of NL-DT5R was inferior to that of SIVmac239 both *in vitro* and *in vivo* [16,17]. These results indicated that genetic modifications in NL-DT5R were insufficient to confer the ability on the virus to grow efficiently in macaque cells [16–18]. In an attempt to improve growth potential of NL-DT5R, we adapted NL-DT5R and its R5-tropic version NL-DT562 to a CyM derived lymphocyte cell line HSC-F, and found a number of genetic substitutions in viral genomes of adapted viruses [19]. We introduced these mutations and CA h6/7L from SIVmac239 into NL-DT5R, and the resultant clone was designated MN4-5S (Fig. 1) [19]. MN4-5S exhibited enhanced growth potential in CyM both *in vitro* and *in vivo* compared to NL-DT5R [19]. But growth ability of MN4-5S was still lower than that of SIVmac239.

In this study, to further improve replication potential of HIV-1mt, we adapted MN4-5S in macaque cells and identified an adaptive mutation in CA that enhances growth ability in the cells. *In silico* structural modeling of the adaptive mutation predicted that Q110D mutation on helix 6 in CA (CA-Q110D) would promote viral replication in macaque cells. Indeed, a proviral clone carrying CA-Q110D, designated MN4Rh-3, exhibited marked enhancement of growth potential in macaque cells relative to all the other HIV-1mt clones we have constructed (Fig. 1). CyM TRIM5α/TRIMCyp susceptibility assays revealed that MN4Rh-3 completely evades from TRIMCyp restriction but not TRIM5α restriction as observed for the other HIV-1mt clones. While CA-Q110D contributed to neither endowment of further resistance to TRIMCyp nor evasion from TRIM5α restriction, CA-Q110D did lead to enhanced single-cycle infectivity to a macaque cell line compared with the other HIV-1mt clones. Our results here indicate that CA-Q110D accelerates viral growth in macaque cells independently of TRIM5 proteins restriction.

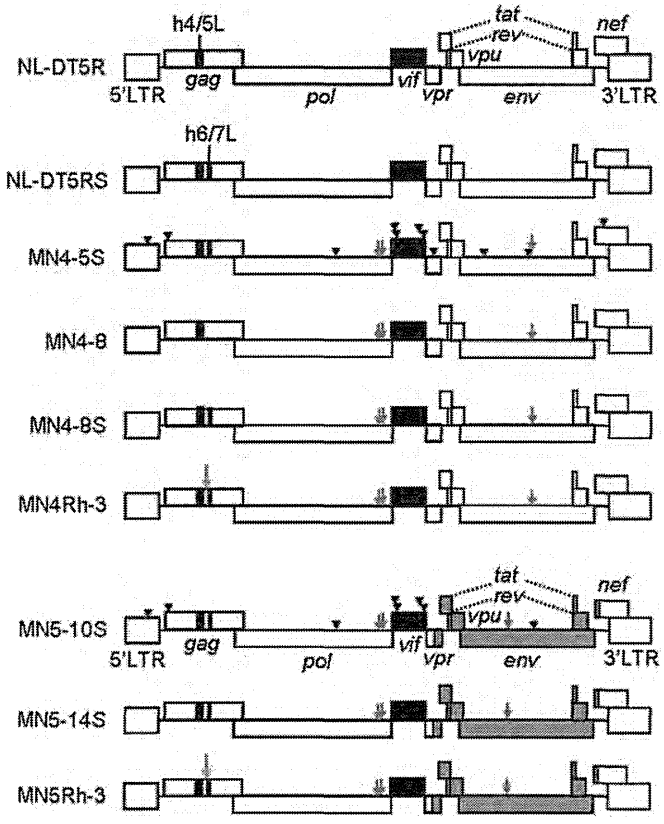

Fig. 1. Proviral genome structure of various HIV-1mt clones used in this study. HIV-1 NL4-3 [26] and SIVmac239 (GenBank: M33262) sequences are indicated by white and black areas, respectively. Gray areas in MN5-10S, MN5-14S and MN5Rh-3 show sequences from NF462 [21]. Blue arrows and black arrowheads show nucleotide substitutions that appeared in viral genomes of NL-DT5R and NL-DT562 during adaptation in HSC-F cells. Among nucleotide substitutions, adaptive mutations that enhance viral growth potential are indicated by blue arrows. Red arrows show the CA-Q110D mutation.

2. Materials and methods

2.1. Plasmid DNA

Construction of NL-DT5R, NL-DT562, NL-DT5RS, and MN4-5S were described previously [16,19–21]. MN4-5S carries all nucleotide substitutions that are present in adapted NL-DT5R and NL-DT562 clones except for mutations in the *env* gene of R5-tropic viruses (MN5-10S, MN5-14S, and MN5Rh-3 in Fig. 1) [19]. MN4-8S contains adaptive (growth-enhancing) mutations in MN4-5S but not the other mutations. MN4Rh-3 was constructed by introduction of the CA-Q110D mutation into MN4-8S. To construct R5-tropic viruses, 3′ halves of viral genomes (*Eco*RI in *vpr* to *Sph*I at the 3′ end of viral genome) of MN4-5S, MN4-8S, and MN4Rh-3 were replaced with the corresponding regions of adapted-NL-DT562,

and were designated MN5-10S, MN5-14S, and MN5Rh-3, respectively. For single-cycle infectivity assays to monitor viral susceptibility to TRIM5 proteins and to determine infectivity for CyM cells, *env*-deficient HIV-1mt variants encoding luciferase gene were constructed. NL-DT5R was cleaved with *Nde*I and *Nhe*I (both sites in *env* gene), blunt ended by T4 DNA polymerase, and resealed by T4 DNA ligase. The resultant clone was designated 5RΔEnv. Luciferase gene was then introduced into *nef* gene of 5RΔEnv as described previously [22], and the resultant clone was designated 5RΔEnv + Luc. A fragment containing the 3′ half genome was cut out from the 5RΔEnv + Luc, and introduced into the corresponding region in HIV-1mt variants (DT5R/4-3, NL-DT5RS, MN4-8, MN4-8S, and MN4Rh-3) to generate 5R/4-3ΔEnv + Luc, 5RSΔEnv + Luc, 4-8ΔEnv + Luc, 4-8SΔEnv + Luc, and 4Rh-3ΔEnv + Luc, respectively.

2.2. Cell culture

A human monolayer cell line 293T [23], a feline kidney cell line CRFK (ATCC CCL-94), and a CyM kidney cell line MK.P3(F) (JCRB 0607) were maintained in Eagles's minimal essential medium (MEM) containing 10% heat-inactivated fetal bovine serum (hiFBS). CRFK cells expressing TRIM5α/TRIMCyp were maintained in MEM containing 10% hiFBS and 400 μg/mL G418 (SIGMA). Macaque lymphocyte cell lines, HSC-F [24] and HSR5.4 [25], were maintained in RPMI-1640 medium containing 10% hiFBS. Recombinant human IL-2 (AbD Serotec) was added to the medium (50 units/mL) for maintenance of HSR5.4 cells. A human lymphocyte cell line MT4/CCR5 (MT4 cells stably expressing CCR5) was maintained in RPMI-1640 medium containing 10% hiFBS and 200 μg/mL hyglomycine (SIGMA).

2.3. Virus replication assays

Virus stocks for infection were prepared from 293T cells transfected with proviral clones as described previously [16,19,26]. Virion-associated reverse transcriptase (RT) activity was measured as described previously [16]. HSC-F cells (10^6) were infected with equal RT units of viruses in the presence of IL-2. For infection of MT4/CCR5 cells (10^6), the spinoculation method [27] was used. Viral growth was monitored by RT activity released into the culture supernatants. We assessed the viral growth potential by the peak day of virus production, and if the viral growth kinetics are similar, by the production level on the peak day.

2.4. Generation and characterization of adapted viral clones

MN4-5S and MN5-10S viruses (Fig. 1) prepared from transfected 293T cells were inoculated into HSR5.4 cells (3×10^6) with an equal amount of viruses (5×10^7 RT units). The cultures were maintained in the presence of IL-2, and HSC-F cells were added on day 34 post-infection. The culture supernatants (collected on day 18 post-cocultivation, the peak day of virus production) were inoculated into fresh HSR5.4 cells, and total DNA was extracted from the cells on day 15 post-infection. Integrated proviruses were amplified from total DNA as two overlapping fragments by the polymerase chain reaction (PCR), and amplified products were cloned into MN5-10S as described previously [16]. Viruses were prepared from 293T cells transfected with the resultant clones, and inoculated into HSR5.4 cells. Only one clone exhibited a rapid growth kinetics compared to MN5-10S, and was designated Ad clone-25. To identify an adaptive mutation that enhances growth potential, each mutation found in the genome of Ad clone-25 was introduced into MN5-14S by site-directed mutagenesis (STRATAGENE). For screening, viruses prepared from transfected 293T cells were inoculated into HSC-F cells, and virus replication was monitored by RT activity released into the culture supernatants.

2.5. Molecular modeling of HIV CA N-terminal domain (NTD)

The crystal structure of HIV-1 CA NTD at a resolution of 2.00 Å (PDB code: 1M9C [28]) was taken from the RCSB Protein Data Bank [29]. The three-dimensional (3-D) models of HIV-1 CA NTD were constructed by the homology modeling technique using 'MOE-Align' and 'MOE-Homology' in the Molecular Operating Environment (MOE) (Chemical Computing Group Inc., Quebec, Canada) as described [30–32]. We obtained 25 intermediate models per one homology modeling in MOE, and selected the 3-D models which were the intermediate models with best scores according to the generalized Born/volume integral methodology [33]. The final 3-D models were thermodynamically optimized by energy minimization using an AMBER99 force field [34] combined with the generalized Born model of aqueous solvation implemented in MOE [35]. Physically unacceptable local structures of the optimized 3-D models were further refined on the basis of evaluation by the Ramachandran plot using MOE.

2.6. Single-cycle infectivity assays

To generate CRFK cells expressing CyM TRIMCyp, the cDNA was isolated from HSC-F cells, and expression vector of FLAG-tagged CyM TRIMCyp was constructed as described previously [18]. The sequence of TRIMCyp from HSC-F cells was identical with Mafa TRIMCyp2 (GenBank: FJ609415). CRFK cell lines expressing CyM TRIMCyp were selected by G418 as described previously [18]. Expression and inhibitory effect of the selected cell clones were verified by Western blotting with anti-FLAG antibody (SIGMA) and by infection with vesicular stomatitis virus G protein (VSV-G) pseudotyped 5R/4-3ΔEnv + Luc, respectively. Assays using naïve CRFK, CRFK expressing CyM TRIM5α [18] or CyM TRIMCyp, and MK.P3(F) cells were similarly performed as described previously [36]. VSV-G pseudotyped virus stocks were prepared from 293T cells transfected with individual HIV-1mtΔEnv + Luc clones and pCMV-G (GenBank: AJ318514)

at a molar ratio of 1:1. Naïve CRFK, CRFK expressing TRIM5α/TRIMCyp and MK.P3(F) cells were infected with an equal titer of viruses (to generate approximately 10^7 relative luminescence (RLU) for naïve CRFK cells), and on day 2 post-infection, cells were analyzed for luciferase activity. Assays using recombinant Sendai virus (SeV)-CyM TRIM5α/TRIMCyp expression system were performed as described previously [31].

3. Results

3.1. An adaptive mutation G114E on helix 6 in CA (CA-G114E) enhances viral growth potential in macaque cells

An HIV-1mt variant MN4-5S replicated more slowly than SIVmac239 in macaque cells. In order to improve its growth potential, we carried out virus adaptation in a macaque lymphocyte cell line HSR5.4. Virus adaptation was performed by long-term culture of HSR5.4 cells infected with MN4-5S (X4-tropic) or its R5-tropic version MN5-10S (Fig. 1). Construction of proviral clones from adapted viruses was described in Materials and methods. We obtained only one clone (Ad clone-25) with enhanced growth potential from 100 proviral clones constructed and tested. We sequenced the entire genome of Ad clone-25, and found three non-synonymous mutations in CA (S33N, G114E, and T147A in Fig. 2A) and one synonymous mutation in integrase (IN)(a4943c in Fig. 2A). To identify an adaptive mutation that enhances growth potential, each mutation found in Ad clone-25 was introduced into a parental clone MN5-14S (Fig. 1). MN5-14S carries only growth-promoting mutations in MN5-10S, and the two clones exhibit similar growth potential in macaque cells. Viruses were prepared from 293T cells transfected with MN5-14S, Ad clone-25, or clones carrying individual mutations, and inoculated into HSC-F cells (Fig. 2A). Only one clone carrying CA-G114E exhibited similar growth kinetics to that of Ad clone-25 but not the others. This result indicates that CA-G114E is an adaptive mutation enhancing growth potential of HIV-1mt in macaque cells. This mutation is exactly the same as the previously found adaptive mutation, which enhanced growth of NL-4/5S6/7SvifS virus in human CEM-SS cells [37]. NL-4/5S6/7SvifS virus is a prototype HIV-1mt bearing the same CA with that of MN4-5S.

3.2. Molecular modeling of the CA NTD of HIV-1mt variants suggests that CA-G114E and CA-Q110D mutations have a similar positive effect on viral replication

The amino acid at position 114 is located in CA NTD. To obtain structural insights into impacts of the G114E substitution in order to improve growth capability of HIV-1mt variants in macaque cells, we conducted computer-assisted structural study: we constructed 3-D models of CA NTD of three HIV-1mt variants, CA-G114E, CA-G114Q, and MN4-5S, using homology-modeling technique (see Materials and methods). Main chain folds of the three models were indistinguishable, suggesting that 3-D position and type of side chain are critical

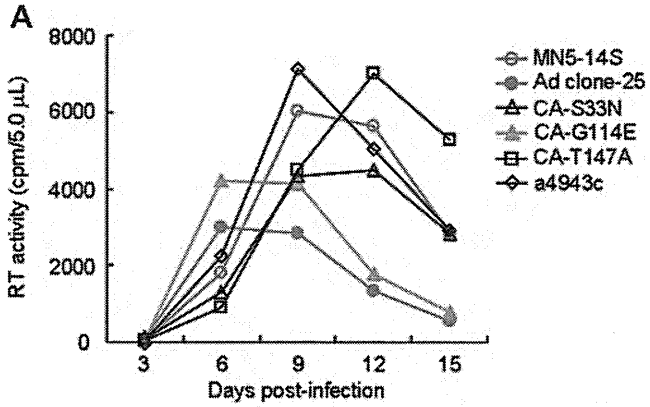

Nucleotide change	Region	Amino acid change in the region
g1283a	CA	S33N
g1526a	CA	G114E
a1624g	CA	T147A
a4943c	IN	None

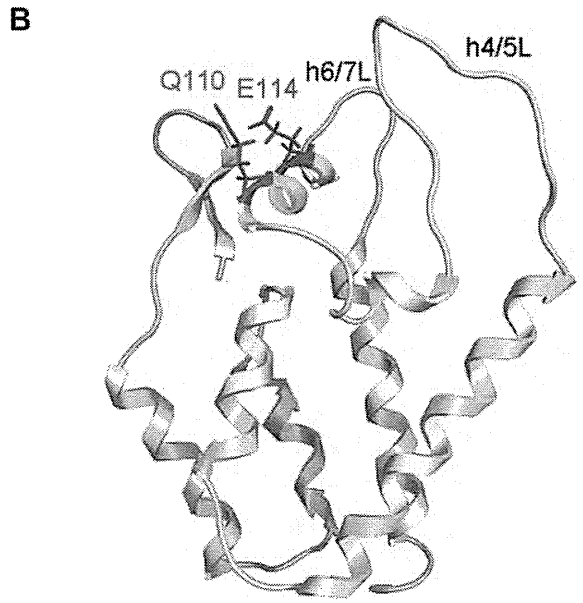

Fig. 2. Mutations in Gag-CA. (A) Identification of an adaptive mutation that enhances viral growth. Nucleotide substitutions found in the genome of Ad clone-25 are indicated at the bottom. Virus samples were prepared from 293T cells transfected with the indicated proviral clones, and equal RT units were inoculated into HSC-F cells. MN5-14S and Ad clone-25 served as controls. Virus replication was monitored by RT activity released into the culture supernatants. (B) 3-D structural models for CA NTD of HIV-1mt variants. Structural models of CA NTD of HIV-1mt variants were constructed by homology-modeling using "MOE-Align" and "MOE-Homology" in MOE as described previously [30–32]. Crystal structure of HIV-1 CA NTD at a resolution of 2.00 Å (PDB code: 1M9C [28]) was used as template for homology modeling. Main chain folds were indistinguishable among the models, and only the model of G114E CA is shown as a representative. Magenta and red sticks: side chains of 110th and 114th amino acid residues, respectively, of the G114E CA NTD.

for the phenotypic change. The modeling study revealed that 114th residue of G114E CA NTD is located on helix 6 in CA NTD such that its side chain protrudes into the exposed surface of CA (Fig. 2B). A charged amino acid residue on a protein surface participates in determining physicochemical properties of interaction surface of the protein and thus influences its structural and functional properties. Therefore, we assumed that the protrusion of a negatively charged side chain from helix 6 into exposed surface could have somehow a positive effect on growth capability of the HIV-1mt variants in macaque cells. In this regard, especially worth noting is that 110th amino acid residue on helix 6 of the HIV-1mt variant CAs was positioned on the same helical face with 114th amino acid residue (Fig. 2B). Therefore, we predicted that substitution of glutamine (Q) at position 110 by acidic amino acid such as aspartic acid (D) and glutamic acid (E) may also have a positive effect on growth capability of the HIV-1mt variants in macaque cells as G114E does. SIVmac239 has aspartic acid and glutamine at the positions 110 and 114, respectively.

3.3. CA-Q110D promotes viral growth more efficiently in macaque cells than CA-G114E mutation but its enhancing effect is species-specific

To confirm our prediction described above, CA-Q110D mutation was introduced into MN5-14S (designated MN5Rh-3), and the growth property in HSC-F cells of MN5Rh-3 and a viral clone carrying G114E (CA-G114E in Fig. 2A) was compared. As shown in Fig. 3A, MN5Rh-3 grew better than CA-G114E, indicating that CA-Q110D further accelerates HIV-1mt replication in macaque cells compared with an adaptive CA-G114E mutation. We next constructed an X4-tropic proviral clone carrying the CA-Q110D (designated MN4Rh-3) (Fig. 1), and compared its growth property with MN5Rh-3 in HSC-F cells (Fig. 3B). MN4Rh-3 was found to exhibit higher growth ability than MN5Rh-3, and was therefore used for infection experiments hereafter.

While CypA and TRIM5α have inhibitory effect on HIV-1 replication in macaque cells, CypA promotes HIV-1 infection in human cells and human TRIM5α only weakly inhibits HIV-1 replication [38–40]. Since the CA-Q110D mutation (acquisition of negatively charged side chain), as predicted by structural modeling, could impact on the interaction of HIV-1 CA and its binding factor(s) by altering physicochemical properties of CA binding surface, it can be speculated that CA-Q110D may promote viral replication specifically in macaque cells. Thus, we analyzed the effect of CA-Q110D on viral growth in macaque and human cells. In this experiment, we used HIV-1mt variants (MN4-8, MN4-8S, and MN4Rh-3) that have distinct CA structures (Fig. 1). Viruses prepared from transfected 293T cells were inoculated into macaque HSC-F and human MT4/CCR5 cells, and examined for growth property (Fig. 3C). The introduction of SIVmac239 CA h6/7L (MN4-8S) resulted in enhanced and reduced viral growth in macaque and human cells, respectively, relative to MN4-8. MN4Rh-3 grew clearly better in macaque cells relative to MN4-8 and MN4-8S, but more poorly in human cells than the other twos. These results demonstrate that the CA-Q110D mutation enhances viral replication in a host cell species-specific manner.

3.4. CA-Q110D does not contribute to evasion from CyM TRIM5 proteins restriction

We predicted that the growth enhancement by CA-Q110D may come from the increased resistance to CyM TRIM5 proteins, and therefore examined the susceptibility of HIV-1mt variants to them by two independent assays.

First, assays were performed in feline kidney CRFK cells expressing TRIM5α or TRIMCyp by using VSV-G pseudotyped viruses encoding the luciferase gene (Fig. 4A–C). The sequence differences between HIV-1mt variants reside only in CA and IN (Figs. 1 and 4). Since adaptive mutations in IN contribute to enhancement of virion production but not early replication phase (manuscript in preparation), only the difference in CA affects the relative single cycle infectivity in this assay. A pseudotyped virus 5R/4-3 carries HIV-1 (NL4-3) CA without any modifications and served as negative control. While 5R and 4-8 have an identical CA structure carrying h4/5L from SIVmac239, 5RS and 4-8S have both h4/5L and h6/7L from SIVmac239 CA. 4Rh-3 carries CA-Q110D mutation in addition to h4/5L and h6/7L from SIVmac239 CA. Viral infectivity was measured by luciferase activity in infected cells and presented as RLU. Naïve CRFK and CRFK cells expressing TRIM5α were infected with an equal amount of viruses generating 10^7 RLU in naïve cells. As shown in Fig. 4B, the infectivity of 5R and 4-8 for cells expressing CyM TRIM5α was similar to that of a negative control 5R/4-3. However, higher infectivity was observed for 5RS and 4-8S relative to 5R and 4-8. These results were consistent with previous reports that h4/5L and h6/7L in HIV-1 CA are a part of determinant for TRIM5α restriction [20,36]. The sensitivity of 4Rh-3 to TRIM5α was similar to that of 5RS and 4-8S. This indicates that CA-Q110D did not contribute to increase the resistance to TRIM5α. It has been reported that CyM TRIMCyp has the ability to restrict HIV-1 replication [15]. To examine the susceptibility of HIV-1mt variants to TRIMCyp, we generated feline CRFK cells expressing TRIMCyp, and the cells were infected with pseudotyped viruses as described above. As shown in Fig. 4C, all the clones tested were more resistant to a similar extent to TRIMCyp than the control 5R/4-3. In agreement with a previous study showing that elimination of alanine at position 88 within h4/5L of HIV-1 CA confers the resistance on the virus to TRIMCyp [15], our results indicate that the replacement of HIV-1 CA h4/5L with that of SIVmac239 is sufficient for HIV-1mt to evade from the TRIMCyp restriction. Second, we performed another susceptibility assay using the recombinant SeV expression system. This system assures a very high expression level of target proteins in cells infected with the recombinant SeV. Therefore, the ability of viruses to completely counteract the restriction effect of TRIM5 proteins could be determined by MT4/SeV-TRIM5 expression system. Human MT4 cells were infected with recombinant SeV expressing CyM TRIM5α, TRIMCyp, or SPRY(−)TRIM5, and then super-infected with HIV-1

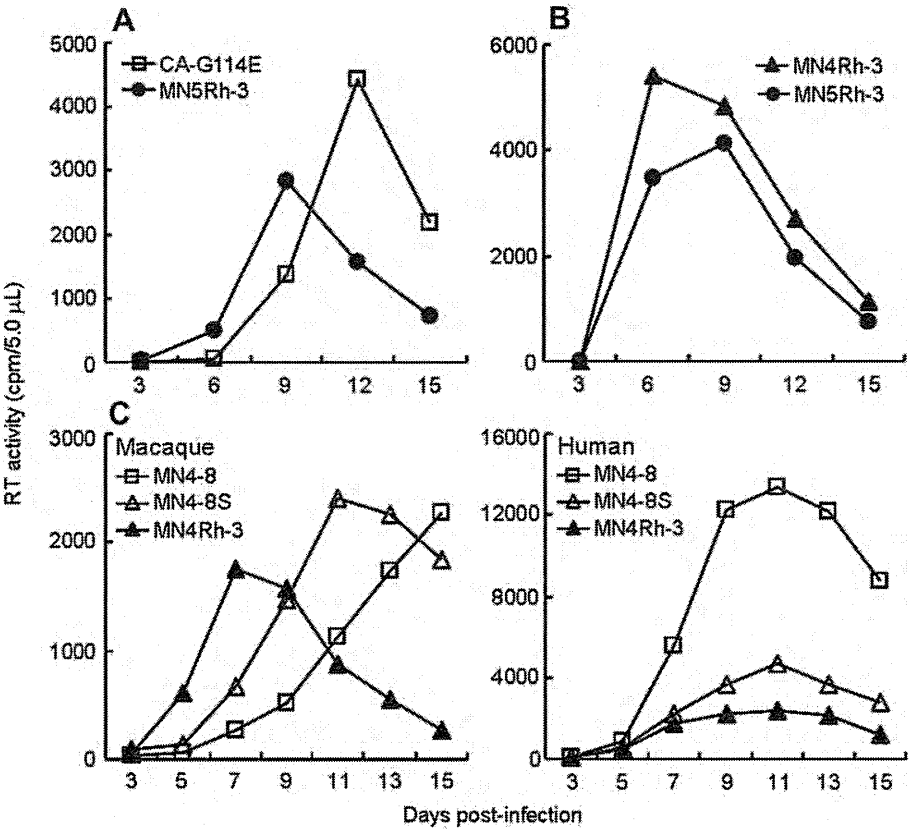

Fig. 3. Effect of CA modification on viral growth in macaque and human lymphocyte cell lines. (A and B) Growth kinetics of HIV-1mt clones carrying CA-G114E or CA-Q110D (MN5Rh-3 and MN4Rh-3) in CyM HSC-F cells. Virus samples were prepared from 293T cells transfected with the indicated proviral clones, and equal amounts (5×10^5 RT units) were inoculated into HSC-F cells (10^6). Virus replication was monitored by RT activity released into the culture supernatants. (C) Growth kinetics of MN4-8, MN4-8S, and MN4Rh-3 in HSC-F (Macaque) and MT4/CCR5 (Human) cells. Virus samples were prepared from 293T cells transfected with the indicated proviral clones, and equal amounts (10^6 RT units) were inoculated into HSC-F cells (10^6). For spinoculation of MT4/CCR5 cells (10^6), 6×10^5 RT units were used as inocula. Virus replication was monitored by RT activity released into the culture supernatants.

(NL4-3), SIVmac239, or HIV-1mt variants. SPRY(−)TRIM5 which can not bind to viral CA served as control. NL4-3 and SIVmac239 also served as controls for viral replication. As shown in Fig. 4D, NL4-3 replicated in cells expressing SPRY(−)TRIM5, but not in TRIM5α and TRIMCyp expressing cells. SIVmac239 exhibited similar growth kinetics in SPRY(−)TRIM5, TRIM5α and TRIMCyp expressing cells. All HIV-1mt variants replicated in TRIMCyp expressing cells similarly well in SPRY(−)TRIM5 cells. Together with assays in CRFK cells, these results showed that all HIV-1mt variants except for 5R/4-3 completely evade from TRIMCyp restriction. In contrast, the growth of all HIV-1mt variants was inhibited in CyM TRIM5α expressing MT4 cells. These results indicate that HIV-1mt variants do not evade from TRIM5α restriction as effectively as SIVmac239.

Results obtained by our two assay systems with respect to the susceptibility of HIV-1mt variants to CyM TRIM5α were apparently different (Fig. 4B and D), but this difference is most likely to be due to the TRIM5α expression level. In MT4 cells infected with recombinant SeV, TRIM5α is expressed at much higher level than that in transduced CRFK cells, masking the increase of resistance to TRIM5α detectable by the transduced CRFK system (Fig. 4B). Indeed, the growth enhancement of 5RS relative to 5R [20] can be explained by the results in Fig. 4B but not those in Fig. 4D. The apparent discrepancy of the sensitivity depending on TRIM5α expression level was also observed between B-LCL cells and transduced CRFK cells [41]. In sum, we can conclude here that MN4Rh-3 exhibits a partial resistance to TRIM5α insufficient for complete evasion as 5RS and 4-8S do, and that the CA-Q110D mutation is irrelevant to this property.

3.5. CA-Q110D enhances viral infectivity for macaque cells

Results so far showed that CA-Q110D does not contribute to evasion from TRIM5 proteins restriction in rather artificial systems using feline and human cells (Fig. 4). To investigate further how CA-Q110D enhances viral replication, we examined single-cycle viral infectivity in macaque cells. CyM kidney MK.P3(F) cells, which have heterozygote for TRIM5α and TRIMCyp, were infected with various VSV-G pseudoviruses and analyzed for their infectivity as described above. As shown in Fig. 5A, viral infectivity was increased by modification of h4/5L (compare 5R/4-3 and 5R&4-8). Modification of h6/7L in addition to h4/5L further augmented viral infectivity (compare 5R&4-8 and 5RS&4-8S). Introduction of the CA-Q110D mutation into 4-8S clone gave the highest infectivity among the viruses tested (see 4Rh-3). The results in

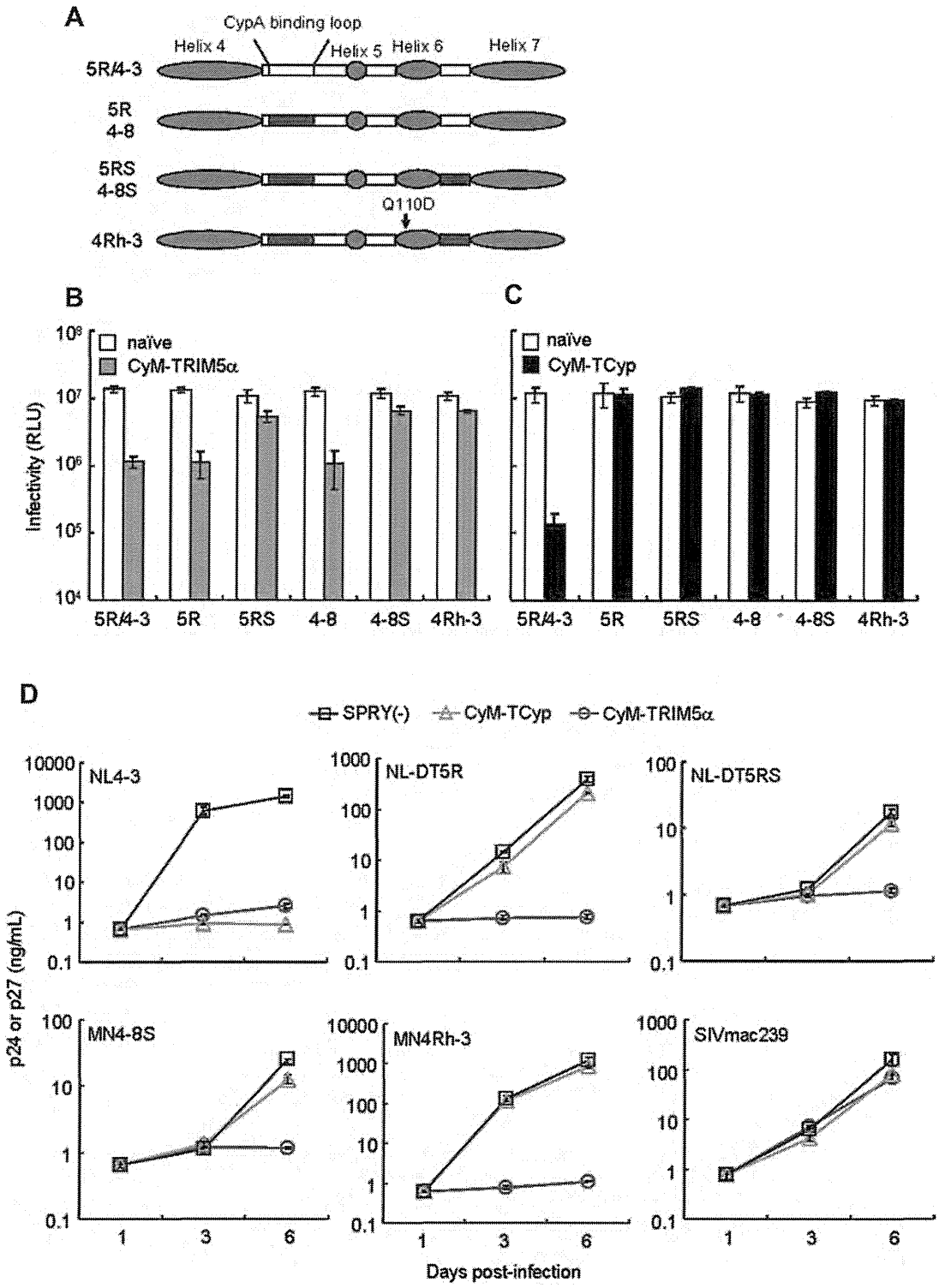

Fig. 4. Effect of CA modification in HIV-1mt variants on viral infectivity. (A) CA structure of viral clones used in TRIM5α/TRIMCyp susceptibility assays. Blue and white areas show helices and loops from HIV-1 NL4-3 CA, respectively. Sequences from SIVmac239 are indicated by black areas. (B and C) Susceptibility of HIV-1mt variants to CyM TRIM5 proteins as examined by CRFK system. Results for CyM TRIM5α (B) and for CyM TRIMCyp (TCyp) (C) are shown. VSV-G pseudotyped viruses were prepared from transfected 293T cells as input samples. Viruses generating 10^7 RLU in CRFK-naïve cells were inoculated into CRFK cells that express CyM TRIM5α or CyM TCyp. On day 2 post-infection, cells were analyzed for luciferase activity by a luminometer. (D) Susceptibility of HIV-1mt variants to CyM TRIM5 proteins as examined by SeV system. Human MT4 cells (10^5) were infected with recombinant SeV expressing CyM TRIM5α, TRIMCyp, or SPRY (−) TRIM5. Nine hours after infection, cells were super-infected with 20 ng (Gag-p24) of HIV-1 NL4-3, various HIV-1mt clones, or 20 ng (Gag-p27) of SIVmac239. Virus replication was monitored by the amount of Gag-p24 from NL4-3 and HIV-1mt clones or Gag-p27 from SIVmac239 in the culture supernatants. Error bars show actual fluctuations between duplicate samples. Data from one representative of three independent experiments are shown.

Fig. 5A show that CA-Q110D uniquely increases viral infectivity in macaque cells not observed in the other experimental systems (Fig. 4), and suggest that some factor(s) in CyM cells other than TRIM5α and TRIMCyp proteins is associated with this enhancement.

As shown in Fig. 5B, MN4Rh-3 displayed slower growth kinetics relative to those of SIVmac239 (note the peak day of virus production), although it grew better than the other HIV-1mt clones in CyM HSC-F cells. Approximately 100-fold more input virus (RT units) compared to SIVmac239 was required for MN4Rh-3 to exhibit similar growth kinetics with SIVmac239 (data not shown). These results have shown that even MN4Rh-3 grows more poorly in macaque cells than a standard SIVmac clone pathogenic for macaque monkeys.

4. Discussion

In this study, we have demonstrated that a single CA mutation (Q110D) greatly promotes HIV-1mt growth in macaque cells (Fig. 3). This enhancing effect was afforded independently of TRIM5 proteins restriction. The virus carrying the CA-Q110D mutation (MN4Rh-3) certainly overcame the anti-viral action of CyM TRIMCyp but not completely CyM TRIM5α. However, the mutation itself (Fig. 1) did not influence anti-TRIMCyp/TRIM5α activity of MN4Rh-3 reported here (Fig. 4). Notably, this mutation exquisitely enhanced viral growth in macaque cells (Fig. 3) by augmenting viral single-cycle infectivity (Fig. 5). The viral growth enhancement reported here is well reproduced in CyM peripheral blood mononuclear cells and in CyMs (manuscript in preparation).

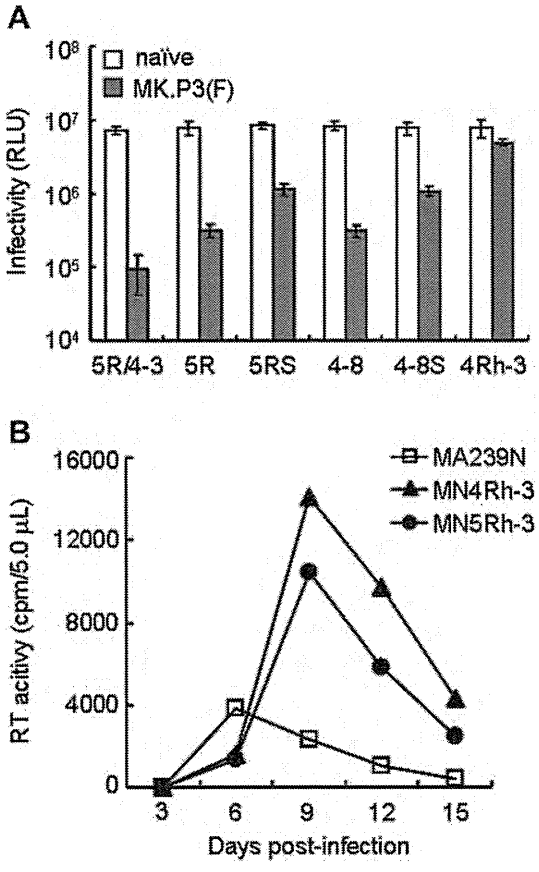

Fig. 5. Replication ability of various viruses in CyM cells. (A) Single-cycle infectivity of various HIV-1mt clones in CyM kidney MK.P3(F) cells. VSV-G pseudotyped viruses indicated were prepared from transfected 293T cells. MK.P3(F) cells were infected with an equal titer of viruses giving 10^7 RLU in CRFK-naïve cells. On day 2 post-infection, cells were analyzed for luciferase activity by a luminometer. (B) Multi-cycle growth kinetics of SIVmac and HIV-1mt viruses in CyM lymphocyte HSC-F cells. Virus samples were prepared from 293T cells transfected with the indicated proviral clones, and equal amounts (10^4 RT units) were inoculated into HSC-F cells (10^6). Virus replication was monitored by RT activity released into the culture supernatants. MA239N, an infectious clone of SIVmac239 with *nef*-open.

Regarding the mechanism for enhancement of viral growth by CA-Q110D, we initially thought a possibility that CA-Q110D compensates the disadvantage in HIV-1mt genome resulted from replacement of HIV-1 CA h4/5L and h6/7L with those of SIVmac239. However, this is highly unlikely because the enhancing effect is macaque cell-dependent (Fig. 3). Most feasible explanation is that CA-Q110D contributes to evade from a negative factor(s) in macaque cells such as CypA. Because HIV-1mt CA was designed not to bind to CypA, and the interaction between the two molecules was indeed undetectable by monitoring CypA virion-incorporation [18,20], we analyzed the binding by computer-assisted structural modeling. Homology modeling of the CA-CypA complexes was performed based on the crystal structure of HIV-1 CA NTD bound to CypA (PDB code: 1M9C [28]), and the binding energies, E_{bind}, were calculated using MOE as described previously [42,43]. As shown in Fig. 6, HIV-1 (NL4-3) CA was predicted to interact with CypA via its h4/5L (binding energy: −64.4 kcal/mol). The binding energy of CA and CypA was decreased by CA modifications, such as h4/5L replacement (NL-DT5R: −31.0 kcal/mol), h4/5L and h6/7L replacement (NL-DT5RS: −36.1 kcal/mol), and Q110D substitution in addition to h4/5L and h6/7L replacement (MN4Rh-3: −30.1 kcal/mol). Decrease in E_{bind} in NL-DT5R is consistent with the result that the h4/5L region directly interacts with CypA [28]. Notably, the E_{bind} for the NL-DT5RS CA was greater than that of the NL-DT5R and MN4Rh-3 CAs. These results suggest that not only h6/7L replacement but also Q110D substitution can influence structure of CypA binding surface of CA. The Q110D substitution is located on the exposed surface of helix 6 connecting to the h6/7L (Fig. 2B). CA helix 6 has been reported to interact with CypA binding region on h4/5L through hydrogen bonding [44,45]. Thereby it is reasonable that the local electrostatic change on the helix 6 by the Q110D substitution influenced structures of h4/5L via changes in fluctuation and conformation of h6/7L. This in turn could lead to reduction in stability of the MN4Rh-3 CA-CypA complex compared with NL-DT5RS CA-CypA complex, as predicted in Fig. 6. Our computer-assisted structural study suggests that the Q110D substitution can induce electrostatic modulation of the overall CA surface structure including h4/5L and h6/7L. Similar modulation mechanism of binding surface structures via charged amino acid substitution at distant site from the binding surface has been reported for Cyp domain of CyM TRIMCyp [15] and CD4 binding site of HIV-1 gp120 outer

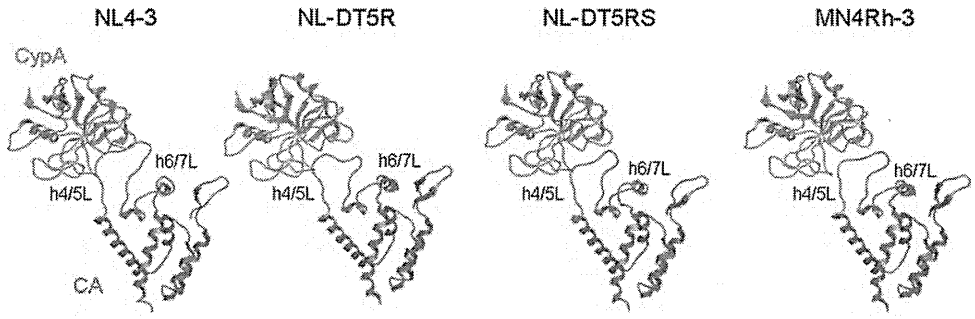

	NL4-3	NL-DT5R	NL-DT5RS	MN4Rh-3
CA	HIV-1 CA	h4/5L from SIVmac239	h4/5L and h6/7L from SIVmac239	h4/5L and h6/7L from SIVmac239 and Q110D
Binding energy (kcal/mol)	-64.447	-31.012	-36.071	-30.051

Fig. 6. Structural models of HIV CA NTD bound to CypA. The model of CA NTD bound to CypA was constructed by homology modeling using the crystal structure of HIV-1 CA NTD and CypA complex (PDB code: 1M9C [28]). The binding energies, E_{bind} (kcal/mol), of the complex were calculated using MOE as described previously [42,43]. The formula $E_{bind} = E_{complex} - (E_{CA} + E_{CypA})$ was used for the E_{bind} calculation, where $E_{complex}$ is the energy of the CA/CypA complex models, E_{CA} is the energy of the CA monomer model, and E_{CypA} is the energy of the CypA monomer model.

domain [46]. Thus, it is not unreasonable to assume that the replication of MN4Rh-3 carrying CA-Q110D is enhanced in macaque cells but reduced in human cells by augmenting its dissociation from CypA (Fig. 6). However, it was found to be difficult to experimentally confirm this structural insight by determining the effect of cyclosporine A or of siRNA against CypA on viral infectivity because interaction between the HIV-1mt CA and CypA was so weak. Alternatively, CA-Q110D may contribute to the alteration of the affinity to unknown anti-CA factor(s) other than CypA and TRIM5 proteins. In this case, it is speculated that the factor(s) might act negatively on HIV-1 replication in macaque cells but positively in human cells, and vice versa. Further study is required to elucidate the mechanism for enhancement of viral growth potential by CA-Q110D.

In conclusion, further modification of the HIV-1mt genome is necessary to overcome unconquered replication block(s) present in macaque cells and obtain viral clones similarly replication-competent in macaque cells and pathogenic for animals with SIVmac (Fig. 5). Considering the genome structure of MN4Rh-3 and the results presented here, major targets for modification now are *gag*-CA (against TRIM5α) and *vpu* (against tetherin). Gag-CA is one of the two principal viral determinants (CA and Vif) for the HIV-1 species-tropism. Construction of HIV-1 CA that evades from TRIM5α restriction is also useful for elucidation of the less-defined CA-TRIM5α interaction and antiviral mechanism of TRIM5α. Tetherin, identified as anti-virion release factor, is antagonized by Vpu [47,48], but macaque tetherin was not counteracted by HIV-1 Vpu [49]. Construction of HIV-1 Vpu that down-modulate macaque tetherin may enhance viral replication *in vivo* as well as *in vitro* [50]. Through these approaches, we may be able to precisely analyze HIV-1 replication and pathogenesis *in vivo* and provide new strategies against HIV-1/AIDS.

Acknowledgments

This study was supported by a grant from the Ministry of Health, Labor and Welfare of Japan (Research on HIV/AIDS project no. H23-003).

References

[1] M.H. Malim, M. Emerman, HIV-1 accessory proteins–ensuring viral survival in a hostile environment, Cell Host Microbe 3 (2008) 388–398.
[2] F. Kirchhoff, Immune evasion and counteraction of restriction factors by HIV-1 and other primate lentiviruses, Cell Host Microbe 8 (2010) 55–67.
[3] R. Shibata, H. Sakai, M. Kawamura, K. Tokunaga, A. Adachi, Early replication block of human immunodeficiency virus type 1 in monkey cells, J. Gen. Virol. 76 (1995) 2723–2730.
[4] M. Nomaguchi, N. Doi, K. Kamada, A. Adachi, Species barrier of HIV-1 and its jumping by virus engineering, Rev. Med. Virol. 18 (2008) 261–275.
[5] M. Nomaguchi, A. Adachi, Virology as biosystematics: towards understanding the viral infection biology, Front. Microbiol. 1 (2010) 2.
[6] R.K. Holmes, M.H. Malim, K.N. Bishop, APOBEC-mediated viral restriction: not simply editing? Trends Biochem. Sci. 32 (2007) 118–128.
[7] H. Huthoff, G.J. Towers, Restriction of retroviral replication by APOBEC3G/F and TRIM5alpha, Trends Microbiol. 16 (2008) 612–619.
[8] K. Strebel, J. Luban, K.T. Jeang, Human cellular restriction factors that target HIV-1 replication, BMC Med. 7 (2009) 48.
[9] J. Luban, Cyclophilin A, TRIM5, and resistance to human immunodeficiency virus type 1 infection, J. Virol. 81 (2007) 1054–1061.
[10] G.J. Towers, The control of viral infection by tripartite motif proteins and cyclophilin A, Retrovirology 4 (2007) 40.
[11] E.E. Nakayama, T. Shioda, Anti-retroviral activity of TRIM5 alpha, Rev. Med. Virol. 20 (2010) 77–92.
[12] R.M. Newman, L. Hall, M. Connole, G.L. Chen, S. Sato, E. Yuste, W. Diehl, E. Hunter, A. Kaur, G.M. Miller, W.E. Johnson, Balancing selection and the evolution of functional polymorphism in old world monkey TRIM5alpha, Proc. Natl. Acad. Sci. U. S. A. 103 (2006) 19134–19139.
[13] S.J. Wilson, B.L. Webb, L.M. Ylinen, E. Verschoor, J.L. Heeney, G.J. Towers, Independent evolution of an antiviral TRIMCyp in rhesus macaques, Proc. Natl. Acad. Sci. U. S. A. 105 (2008) 3557–3562.

[14] A.J. Price, F. Marzetta, M. Lammers, L.M. Ylinen, T. Schaller, S.J. Wilson, G.J. Towers, L.C. James, Active site remodeling switches HIV specificity of antiretroviral TRIMCyp, Nat. Struct. Mol. Biol. 16 (2009) 1036–1042.
[15] L.M. Ylinen, A.J. Price, J. Rasaiyaah, S. Hué, N.J. Rose, F. Marzetta, L.C. James, G.J. Towers, Conformational adaptation of Asian macaque TRIMCyp directs lineage specific antiviral activity, PLoS Pathog. 6 (2010) e1001062.
[16] K. Kamada, T. Igarashi, M.A. Martin, B. Khamsri, K. Hatcho, T. Yamashita, M. Fujita, T. Uchiyama, A. Adachi, Generation of HIV-1 derivatives that productively infect macaque monkey lymphoid cells, Proc. Natl. Acad. Sci. U. S. A. 103 (2006) 16959–16964.
[17] T. Igarashi, R. Iyengar, R.A. Byrum, A. Buckler-White, R.L. Dewar, C.E. Buckler, H.C. Lane, K. Kamada, A. Adachi, M.A. Martin, Human immunodeficiency virus type 1 derivative with 7% simian immunodeficiency virus genetic content is able to establish infections in pig-tailed macaques, J. Virol. 81 (2007) 11549–11552.
[18] K. Kamada, T. Yamashita, K. Hatcho, A. Adachi, M. Nomaguchi, Evasion from CypA- and APOBEC-mediated restrictions is insufficient for HIV-1 to efficiently grow in simian cells, Microbes Infect. 11 (2009) 164–171.
[19] A. Saito, M. Nomaguchi, S. Iijima, A. Kuroishi, T. Yoshida, Y.J. Lee, T. Hayakawa, K. Kono, E.E. Nakayama, T. Shioda, Y. Yasutomi, A. Adachi, T. Matano, H. Akari, Improved capacity of a monkey-tropic HIV-1 derivative to replicate in cynomolgus monkeys with minimal modifications, Microbes Infect. 13 (2011) 58–64.
[20] A. Kuroishi, A. Saito, Y. Shingai, T. Shioda, M. Nomaguchi, A. Adachi, H. Akari, E.E. Nakayama, Modification of a loop sequence between alpha-helices 6 and 7 of virus capsid (CA) protein in a human immunodeficiency virus type 1 (HIV-1) derivative that has simian immunodeficiency virus (SIVmac239) vif and CA alpha-helices 4 and 5 loop improves replication in cynomolgus monkey cells, Retrovirology 6 (2009) 70.
[21] T. Yamashita, N. Doi, A. Adachi, M. Nomaguchi, Growth ability in simian cells of monkey cell-tropic HIV-1 is greatly affected by downstream region of the vif gene, J. Med. Invest. 55 (2008) 236–240.
[22] M. Yamashita, M. Emerman, Capsid is a dominant determinant of retrovirus infectivity in nondividing cells, J. Virol. 78 (2004) 5670–5678.
[23] J.S. Lebkowski, S. Clancy, M.P. Calos, Simian virus 40 replication in adenovirus-transformed human cells antagonizes gene expression, Nature 317 (1985) 169–171.
[24] H. Akari, T. Fukumori, S. Iida, A. Adachi, Induction of apoptosis in herpesvirus saimiri-immortalized T lymphocytes by blocking interaction of CD28 with CD80/CD86, Biochem. Biophys. Res. Commun. 263 (1999) 352–356.
[25] N. Doi, S. Fujiwara, A. Adachi, M. Nomaguchi, Growth ability in various macaque cell lines of HIV-1 with simian cell-tropism, J. Med. Invest. 57 (2010) 284–292.
[26] A. Adachi, H.E. Gendelman, S. Koenig, T. Folks, R. Willey, A. Rabson, M.A. Martin, Production of acquired immunodeficiency syndrome-associated retrovirus in human and nonhuman cells transfected with an infectious molecular clone, J. Virol. 59 (1986) 284–291.
[27] U. O'Doherty, W.J. Swiggard, M.H. Malim, Human immunodeficiency virus type 1 spinoculation enhances infection through virus binding, J. Virol. 74 (2004) 10074–10080.
[28] B.R. Howard, F.F. Vajdos, S. Li, W.I. Sundquist, C.P. Hill, Structural insights into the catalytic mechanism of cyclophilin A, Nat. Struct. Biol. 10 (2003) 475–481.
[29] N. Deshpande, K.J. Addess, W.F. Bluhm, J.C. Merino-Ott, W. Townsend-Merino, Q. Zhang, C. Knezevich, L. Xie, L. Chen, Z. Feng, R.K. Green, J.L. Flippen-Anderson, J. Westbrook, H.M. Berman, P.E. Bourne, The RCSB protein data bank: a redesigned query system and relational database based on the mmCIF schema, Nucleic Acids Res. 33 (Database issue) (2005) D233–D237.
[30] H. Song, E.E. Nakayama, M. Yokoyama, H. Sato, J.A. Levy, T. Shioda, A single amino acid of the human immunodeficiency virus type 2 capsid affects its replication in the presence of cynomolgus monkey and human TRIM5alphas, J. Virol. 81 (2007) 7280–7285.
[31] K. Kono, H. Song, M. Yokoyama, H. Sato, T. Shioda, E.E. Nakayama, Multiple sites in the N-terminal half of simian immunodeficiency virus capsid protein contribute to evasion from rhesus monkey TRIM5α-mediated restriction, Retrovirology 7 (2010) 72.
[32] N. Inagaki, H. Takeuchi, M. Yokoyama, H. Sato, A. Ryo, H. Yamamoto, M. Kawada, T. Matano, A structural constraint for functional interaction between N-terminal and C-terminal domains in simian immunodeficiency virus capsid proteins, Retrovirology 7 (2010) 90.
[33] P. Labute, The generalized Born/volume integral implicit solvent model: estimation of the free energy of hydration using London dispersion instead of atomic surface area, J. Comput. Chem. 29 (2008) 1693–1698.
[34] J.W. Ponder, D.A. Case, Force fields for protein simulations, Adv. Protein Chem. 66 (2003) 27–85.
[35] A. Onufriev, D. Bashford, D.A. Case, Modification of the generalized Born model suitable for macromolecules, J. Phys. Chem. B 104 (2000) 3712–3720.
[36] T.Y. Lin, M. Emerman, Determinants of cyclophilin A-dependent TRIM5 alpha restriction against HIV-1, Virology 379 (2008) 335–341.
[37] A. Kuroishi, K. Bozek, T. Shioda, E.E. Nakayama, A single amino acid substitution of the human immunodeficiency virus type 1 capsid protein affects viral sensitivity to TRIM5 alpha, Retrovirology 7 (2010) 58.
[38] M. Stremlau, C.M. Owens, M.J. Perron, M. Kiessling, P. Autissier, J. Sodroski, The cytoplasmic body component TRIM5alpha restricts HIV-1 infection in old world monkeys, Nature 427 (2004) 848–853.
[39] Z. Keckesova, L.M. Ylinen, G.J. Towers, Cyclophilin A renders human immunodeficiency virus type 1 sensitive to old world monkey but not human TRIM5 alpha antiviral activity, J. Virol. 80 (2006) 4683–4690.
[40] E. Sokolskaja, L. Berthoux, J. Luban, Cyclophilin A and TRIM5alpha independently regulate human immunodeficiency virus type 1 infectivity in human cells, J. Virol. 80 (2006) 2855–2862.
[41] S.Y. Lim, T. Rogers, T. Chan, J.B. Whitney, J. Kim, J. Sodroski, N.L. Letvin, TRIM5alpha modulates immunodeficiency virus control in rhesus monkeys, PLoS Pathog. 6 (2010) e1000738.
[42] C.O. Onyango, A. Leligdowicz, M. Yokoyama, H. Sato, H. Song, E.E. Nakayama, T. Shioda, T. de Silva, J. Townend, A. Jaye, H. Whittle, S. Rowland-Jones, M. Cotten, HIV-2 capsids distinguish high and low virus load patients in a West African community cohort, Vaccine 28 (2010) B60–B67.
[43] M. Kinomoto, R. Appiah-Opong, J.A. Brandful, M. Yokoyama, N. Nii-Trebi, E. Ugly-Kwame, H. Sato, D. Ofori-Adjei, T. Kurata, F. Barre-Sinoussi, T. Sata, K. Tokunaga, HIV-1 proteases from drug-naive West African patients are differentially less susceptible to protease inhibitors, Clin. Infect. Dis. 41 (2005) 243–251.
[44] R.K. Gitti, B.M. Lee, J. Walker, M.F. Summers, S. Yoo, W.I. Sundquist, Structure of the amino-terminal core domain of the HIV-1 capsid protein, Science 273 (1996) 231–235.
[45] C. Tang, Y. Ndassa, M.F. Summers, Structure of the N-terminal 283-residue fragment of the immature HIV-1 Gag polyprotein, Nat. Struct. Biol. 9 (2002) 537–543.
[46] M. Yokoyama, S. Naganawa, K. Yoshimura, S. Matsushita, H. Sato, Structural dynamics of HIV-1 envelope Gp120 outer domain with V3 loop, PLoS One 7 (2012) e37530.
[47] S.J. Neil, T. Zang, P.D. Bieniasz, Tetherin inhibits retrovirus release and is antagonized by HIV-1 Vpu, Nature 451 (2008) 425–430.
[48] N. Van Damme, D. Goff, C. Katsura, R.L. Jorgenson, R. Mitchell, M.C. Johnson, E.B. Stephens, J. Guatelli, The interferon-induced protein BST-2 restricts HIV-1 release and is downregulated from the cell surface by the viral Vpu protein, Cell Host Microbe 3 (2008) 245–252.
[49] D. Sauter, M. Schindler, A. Specht, W.N. Landford, J. Münch, K.A. Kim, J. Votteler, U. Schubert, F. Bibollet-Ruche, B.F. Keele, J. Takehisa, Y. Ogando, C. Ochsenbauer, J.C. Kappes, A. Ayouba, M. Peeters, G.H. Learn, G. Shaw, P.M. Sharp, P. Bieniasz, B.H. Hahn, T. Hatziioannou, F. Kirchhoff, Tetherin-driven adaptation of Vpu and Nef function and the evolution of pandemic and nonpandemic HIV-1 strains, Cell Host Microbe 6 (2009) 409–421.
[50] M. Shingai, T. Yoshida, M.A. Martin, K. Strebel, Some human immunodeficiency virus type 1 Vpu proteins are able to antagonize macaque BST-2 in vitro and in vivo: Vpu-negative simian-human immunodeficiency viruses are attenuated in vivo, J. Virol. 85 (2011) 9708–9715.

ELSEVIER

Institut Pasteur

Microbes and Infection 15 (2013) 319–328

www.elsevier.com/locate/micinf

Original article

Systemic biological analysis of the mutations in two distinct HIV-1mt genomes occurred during replication in macaque cells

Masako Nomaguchi [a], Naoya Doi [a], Sachi Fujiwara [a], Akatsuki Saito [b], Hirofumi Akari [b], Emi E. Nakayama [c], Tatsuo Shioda [c], Masaru Yokoyama [d], Hironori Sato [d], Akio Adachi [a,*]

[a] *Department of Microbiology, Institute of Health Biosciences, The University of Tokushima Graduate School, 3-18-15 Kuramoto, Tokushima 770-8503, Japan*
[b] *Center for Human Evolution Modeling Research, Primate Research Institute, Kyoto University, Aichi, Japan*
[c] *Department of Viral Infections, Research Institute for Microbial Diseases, Osaka University, Osaka, Japan*
[d] *Laboratory of Viral Genomics, Pathogen Genomics Center, National Institute of Infectious Diseases, Tokyo, Japan*

Received 17 December 2012; accepted 24 January 2013
Available online 4 February 2013

Abstract

Fundamental property of viruses is to rapidly adapt themselves under changing conditions of virus replication. Using HIV-1 derivatives that poorly replicate in macaque cells as model viruses, we studied here mechanisms for promoting viral replication in non-natural host cells. We found that the HIV-1s could evolve to grow better in both macaque and human cells by the continuous culture in macaque lymphocyte cell lines. Notably, only several mutations at defined sites of the Pol-integrase and/or the Env-gp120 reproducibly appeared in repeated adaptation experiments and were sufficient to cause the phenotypic change. Meanwhile, no amino acid changes to enhance viral replication in macaque cells were found in interaction sites for the known anti-retroviral proteins. These findings disclose a hitherto unappreciated evolutionary pathway to augment HIV-1 replication in primate cells, where tuning of viral interactions with positive rather than negative factors for replication can play a dominant role.

Keywords: HIV-1; HIV-1mt; Pol-IN; Env-gp120; Adaptive mutation; Macaque cells

1. Introduction

Viruses evolve extremely rapidly under the changing conditions of virus replication. HIV-1 is no exception. HIV-1 possesses high adaptation potential due to the ability to acquire sequence alterations through high mutation rate of reverse transcriptase (RT) and recombination of viral genomes [1,2]. Change of viral properties by genetic alterations leads to resistance to antiviral drugs, escape from host immune system, and adaptation to new hosts upon transmission [3–6]. Experimental approaches that analyze the genomic change and evolution of viruses are commonly used effective measures to know how viruses adapt themselves under a certain selective pressure. Such studies, however, usually have focused on genetic changes in a limited and selected region of viral genomes or sequence variations in a specified mass of virus.

HIV-1 does not replicate in most animal species including rodents and macaques. Inhibition of HIV-1 replication in macaque cells, at least in part, is mediated by host restriction factors such as APOBEC3 proteins, cyclophilin A (CypA), TRIM5α/TRIMCyp (TRIM5 proteins), and tetherin (for review, refer to references [7–10]). Encounters with pathogenic viruses impose selective pressure on restriction factors, and influence their antiviral specificity [11–13]. Even though human cells also have orthologs of these factors, HIV-1 evades their restriction and replicates well in humans. This suggests that both viruses and host cells co-evolve under the mutual selective pressure. Thus, evolution of viruses is determined by adaptation potential of viruses and their interaction with host cells.

* Corresponding author. Tel.: +81 88 633 7078; fax: +81 88 633 7080.
E-mail address: adachi@basic.med.tokushima-u.ac.jp (A. Adachi).

1286-4579/$ - see front matter © 2013 Institut Pasteur. Published by Elsevier Masson SAS. All rights reserved.
http://dx.doi.org/10.1016/j.micinf.2013.01.005

Prototype macaque cell-tropic HIV-1 (pHIV-1mt), NL-DT5R (5R; X4-tropic) and NL-DT562 (562; R5-tropic), carry a small portion of *gag* gene and an entire *vif* gene from SIVmac239 (Fig. 1). These viruses are insufficiently infectious for macaque cells by their partial resistance to CypA/TRIM5 proteins and evasion from APOBEC3G/F restriction, and their replication potentials were significantly lower than that of pathogenic SIVmac239 [14–16]. These results indicate that macaque cells still impose strong restrictive pressure on pHIV-1mt replication. Therefore, clones 5R and 562 are suitable materials to analyze what genetic changes they would acquire and how they would adapt themselves to environments within macaque cells. As experimental approach to do this, we have performed virus adaptation experiments by the long-term culture of 5R- or 562-infected macaque cells, and successfully obtained adapted viruses with enhanced growth ability [17]. In this study, we inquired into the biological relevance of mutations that appeared in the genomes of adapted viral clones by investigating thoroughly the effect of mutations on viral growth. Although a number of genetic substitutions were found in the genomes of adapted viruses, mutations in *pol*-integrase (IN) and *env*-gp120 only were found to be responsible for enhancement of viral replication. Extensive and repeated virus adaptation experiments revealed that viral clones with augmented growth potential are characterized by acquisition of adaptive mutations in *pol*-IN and in *env*-gp120. Our results suggest that pHIV-1mt evolves in a certain adaptation pathway under the restrictive and uniform environments imposed by macaque cells, and that genetic alterations do not always have biological significance for escaping selective pressure, supporting Kimura's neutral theory of molecular evolution [18].

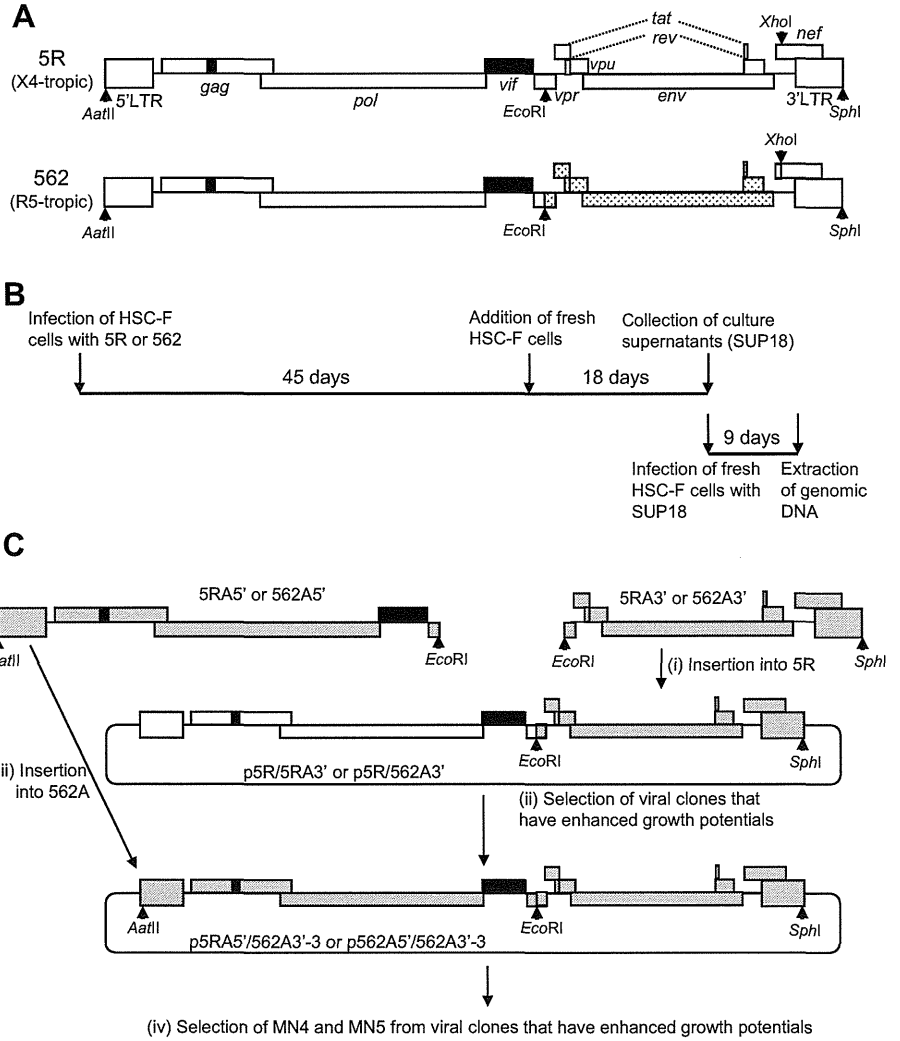

Fig. 1. Molecular cloning of viral genomes from macaque cell-adapted viruses. (A) Genome structure of 5R and 562 [14,16]. Sequence from NF462 [32] is shown by dotted areas. Black areas show the regions derived from SIVmac239. (B) Schedule of virus adaptation and the harvest of adapted viruses [17]. Genomic DNA prepared from infected cells for molecular cloning is indicated. (C) Generation and selection of proviral clones from adapted 5R and 562 viruses. The procedure starts with (i) and ends with (iv). For details, see Materials and methods. PCR amplified fragments derived from adapted 5R (5RA) or adapted 562 (562A) are shown by gray areas. White and black areas indicate the region from 5R.

2. Materials and methods

2.1. Cells

A human monolayer cell line 293T [19] was cultured in Eagle's MEM supplemented with 10% heat-inactivated FBS (hiFBS). A cynomolgus macaque (CyM) lymphocyte cell line HSC-F [20] and a rhesus monkey (RhM) lymphocyte cell line HSR5.4S1 [21] were maintained in RPMI1640 containing 10% hiFBS (for HSR5.4S1, 50 units/mL of IL-2 (AbD Serotec) were added). Human MT4/CCR5 cells (MT4 cells stably expressing CCR5) were maintained RPMI1640 containing 10% hiFBS and 200 μg/mL of hygromycin B (Sigma–Aldrich).

2.2. Transfection, RT assays and infection

Virus stocks were prepared by transfection of 293T cells with viral clones using the calcium phosphate co-precipitation method [22]. On day 2 post-transfection, culture supernatants were collected and stored at −80 °C until use. Virion-associated RT activity was measured as described previously [23]. HSC-F cells were infected with an equal amount of virus preparations in the presence of IL-2. For infection of MT4/CCR5 cells, the spinoculation method [24] was used. Virus replication was monitored by RT activity in the culture supernatants, and viral growth potentials were evaluated by the peak day of virus production or by the level of virus production on the peak day.

2.3. Plasmid DNAs

Construction of pHIV-1mt clones designated 5R and 562 has been previously described [14,16]. Proviral clones derived from adapted viruses were generated by PCR as described previously [14]. Two rounds of adaptation experiments independently performed are outlined in Figs. 1–4, and their details are described below. Introduction of genetic substitutions was performed by the QuickChange site-directed mutagenesis kit (Agilent Technologies).

2.4. First adaptation experiment

As indicated in Fig. 1, to construct molecular clones of adapted viruses from 5R and 562, CyM HSC-F cells were infected with the culture supernatants collected from long-term cultures. On day 9 post-infection, genomic DNA was extracted from cells, and integrated proviruses were amplified as two overlapping fragments by PCR as described previously [14]. To generate molecular clones that exhibit phenotypes of adapted viruses, we first introduced 3′ half genomes (*Eco*RI site in Vpr to *Sph*I site at 3′ end of the genome) from adapted 5R (5RA) and 562 (562A) viruses into 5R, and the resultant constructs were designated p5R/5RA3′ and p5R/562A3′, respectively. Virus stocks were prepared from 293T cells transfected with p5R/5RA3′ or p5R/562A3′, and inoculated into HSC-F cells. Virus replication was monitored by RT activity released into the culture supernatant. A molecular clone that grows best was selected for 5RA and 562A (p5R/5RA3′-14 and p5R/562A3′-3, respectively). Then, 5′ half genomes (*Aat*II site at the 5′ end of the genome to *Eco*RI site in Vpr) of adapted viruses (5RA5′ and 562A5′) were introduced into the selected clone (p5R/562A3′-3), and the resultant constructs were designated p5RA5′/562A3′-3 and p562A5′/562A3′-3, respectively. Proviral clones with the best replication potential were selected as described above. Finally, proviral clones that have a full-length viral genome derived from adapted 5R and 562 viruses were constructed, and designated MN4 and MN5, respectively (see Fig. 2 for their genome structures).

2.5. Second adaptation experiment

As indicated in Fig. 4, HSC-F (1×10^6) and RhM HSR5.4S1 cells (3×10^6) were infected with 5R or 562 viruses prepared from transfected 293T cells to obtain adapted viruses. Half of the culture medium (5 mL) was replaced every 3 days. Fresh HSC-F (1×10^6) and HSR5.4S1 cells (3×10^6) were added in each long-term culture on day 28 post-infection. Half of the culture medium (5 mL) was replaced every 3 days, and harvested supernatants were stored at −80 °C. HSC-F cells were infected with supernatants collected on day 33 post-infection from 5R- or 562-infected HSC-F long-term cultures. On day 9 and 12 post-infection, genomic DNA was extracted from infected cells. For HSR5.4S1 cultures, supernatants collected from 5R- and 562-infected cultures on day 39 and 42 post-infection, respectively, were inoculated into fresh HSR5.4S1 cells. On day 8 and 11 post-infection, genomic DNA was extracted from infected cultures. Amplification of integrated proviruses from genomic DNA and construction of proviral clones were carried out as described above. Viruses prepared from 293T cells transfected with these proviral clones were inoculated into HSC-F and HSR5.4S1 cells depending on which cells were used for long-term culture. Selection of viral clones with enhanced replication capability was carried out as described above.

3. Results

3.1. Mutations in Pol-IN or Env-gp120 are important for enhancement of pHIV-1mt replication in macaque cells

We previously reported that adapted viruses with enhanced growth potential emerged in prolonged cultures of 5R- or 562-infected macaque (CyM) cells [17]. Genomes of adapted viruses should have some genetic changes to augment their growth ability, and adapted viruses were expected to exist as a mass of viruses with distinct replication potential. To identify an adaptive mutation responsible for enhanced growth potential, it is necessary to construct proviral clones that exhibit a better-growing phenotype. Experimental details for construction are shown in Fig. 1. Of 72 proviral clones constructed, some of them (9 clones) did not produce virions in transfected 293T cells as determined by virion-associated RT activity or were not infectious for a CyM lymphocyte cell line HSC-F as well (16 clones). Finally, we have obtained molecular clones

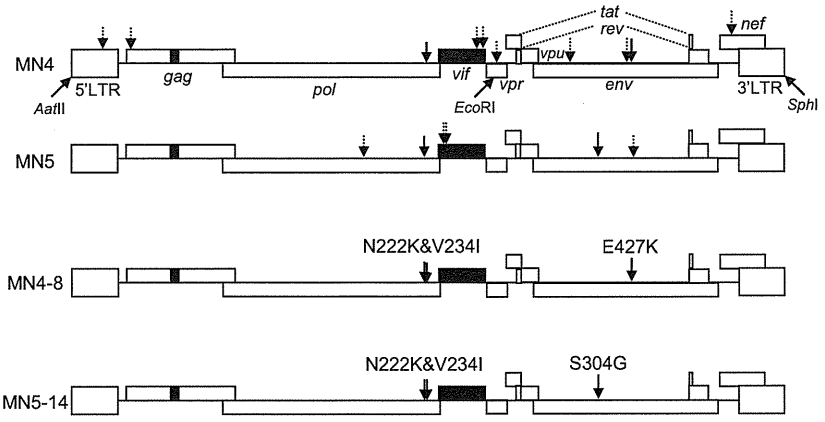

Virus	Genomes from adapted virus	Nucleotide change	Region	Amino acid change in the region
MN4	5' half	t453c	LTR	None
(derived from adapted 5R)	(MN4-5')	g823a	Matrix	E12K
		g4923a	**Pol-IN**	**V234I**
		g5611a	Vif	R171K
		g5693a	Vif	None
	3' half	g5944a	Vpr	None
	(MN4-3')	g6915a	Env-gp120 (V2)	None
		g7606a	Env-gp120 (V4)	E401K
		g7684a	**Env-gp120 (C4)**	**E427K**
		g9191a	Nef	V74I
MN5	5' half	a4049c	Reverse transcriptase	None
(derived from adapted 562)	(MN5-5')	**t4889a**	**Pol-IN**	**N222K**
		g5156a	Vif	None
		t5195a	Vif	None
	3' half	**a7318g**	**Env-gp120 (V3 loop)**	**S304G**
	(MN5-3')	c7812t	Env-gp120 (C5)	None

Fig. 2. Various mutations found in the first adaptation experiment. (Upper) Proviral genome structures of MN4, MN5, and their derivatives. Black areas show the regions derived from SIVmac239. Broken arrows show mutations that appeared during viral adaptation. Solid arrows indicate adaptive mutations in Pol-IN and Env-gp120 that enhance viral growth (Fig. 3). Out of the mutations present in MN4 and MN5, clones MN4-8 and MN5-14 carry the adaptive (growth-enhancing) mutations only. (Lower) Mutations associated with adaptation of 5R and 562 viruses to HSC-F cells. Bold letters show adaptive mutations that are responsible for enhancement of viral replication in cells. 5′ half indicates a fragment from *Aat*II at the 5′ end to *Eco*RI in *vpr* of the viral genome. 3′ half indicates a fragment from *Eco*RI in *vpr* to *Sph*I at the 3′ end of the viral genome.

MN4 and MN5 from adapted 5R and 562 viruses, respectively (Fig. 2).

To identify genetic changes acquired in genomes during virus adaptation, the entire genomes of MN4 and MN5 were sequenced. As shown in Fig. 2, MN4 and MN5 contained ten and six nucleotide substitutions, respectively. To examine the effect of these mutations on viral replication, each mutation was introduced into parental clones 5R and 562 as follows: (i) mutations in MN4 were introduced into 5R; (ii) mutations in 5′ half of MN5 genome were introduced into 5R (5′ half of 562 genome is identical to that of 5R (see Fig. 1A)); (iii) mutations in 3′ half of MN5 genome were introduced into 562. To construct positive control clones for viral growth (Fig. 3), we inserted a half of MN4 and MN5 genomes into the corresponding regions of 5R to generate full-length clones MN4-5′/5R, 5R/MN4-3′, MN5-5′/5R, and 5R/MN5-3′ (Fig. 2). Viruses were then prepared from 293T cells transfected with parental clones, positive controls, or test clones carrying each mutation, and inoculated into HSC-F cells (Fig. 3). MN4-5′ contains five genetic mutations (Fig. 2). Of the five clones examined, only the 5R carrying g4923a (V234I in IN) exhibited a similar growth kinetics to MN4-5′/5R (Fig. 3A). Growth kinetics of 5R carrying the other mutations were similar or slower relative to the parental clone 5R (Fig. 3A). MN4-3′ and MN5-5′ carry five and four nucleotide substitutions, respectively (Fig. 2). A clone that exhibits similar growth kinetics to 5R/MN4-3′ was 5R carrying g7684a